Ca-looping for postcombustion CO_2 capture: A comparative analysis on the performances of dolomite and limestone

J. M. Valverde[a*], P. E. Sanchez-Jimenez[b], L. A. Perez-Maqueda[b]

[a] Faculty of Physics. University of Seville. Avenida Reina Mercedes s/n, 41012 Sevilla, Spain

[b] Instituto de Ciencia de Materiales de Sevilla (C.S.I.C.-Univ. Seville), Americo Vespucio 49, 41092 Sevilla, Spain

[*] **Corresponding author:** Phone no. +34 954550960. Fax no. +34 954239434. Email: jmillan@us.es

Keywords: CO_2 capture; Calcium looping; limestone; dolomite

Abstract

The low cost and wide availability of natural limestone ($CaCO_3$) is at the basis of the industrial competitiveness of the Ca-looping (CaL) technology for postcombustion CO_2 capture as already demonstrated by $\sim$1 Mw_t scale pilot projects. A major focus of studies oriented towards further improving the efficiency of the CaL technology is how to prevent the gradual loss of capture capacity of limestone derived CaO as the number of carbonation/calcination cycles is increased. Natural dolomite ($MgCa(CO_3)_2$) has been proposed as an alternative sorbent precursor to limestone. Yet, carbonation of MgO is not thermodynamically favorable at CaL conditions, which may hinders the capture performance of dolomite. In the work described in this paper we carried out a thermogravimetric analysis on the multicyclic capture performance of natural dolomite under realistic regeneration conditions necessarily implying high calcination temperature, high CO_2 concentration and fast transitions between the carbonation and calcination stages. Our study demonstrates that the sorbent derived from dolomite has a greater capture capacity as compared to limestone. SEM analysis shows that MgO grains in the decomposed dolomite are resistant to sintering under severe calcination conditions and segregate from CaO acting as a thermally stable support which mitigates the multicyclic loss of CaO conversion. Furthermore, full decomposition of dolomite is achieved at significantly lower calcination temperatures as compared to limestone, which would help improving further the industrial competitiveness of the technology.

I. INTRODUCTION

The Ca-looping (CaL) technology has recently emerged as a potentially feasible process for postcombustion CO_2 capture [1–3]. As a main advantage over other technologies it stands the low cost, wide availability and harmlessness towards the environment of natural limestone to be used as CaO precursor for CO_2 capture [4, 5]. In this process, CO_2 is chemisorbed on the surface of CaO particles fluidized in a gas-solid reactor (carbonator) by the postcombustion gas stream at atmospheric pressure and temperatures about 650°C. The solids partially carbonated after typically short residence times (of a few minutes) are circulated into a second gas-solid reactor (calciner) where CaO is regenerated by calcination at atmospheric pressure and a gas stream of highly concentrated CO_2 is retrieved for compression and storage.

The CaL technology is being demonstrated in large-scale pilot plants (up to 1.7 MW_t) showing efficient and sustainable CO_2 capture [3, 6]. A typical run commences by precalcining the initial inventory of limestone in air after which the calciner is set to oxy-combustion mode and the circulation of solids in the loop is started. Burning fuel with pure oxygen (oxy-combustion) ensures a high CO_2 concentration in the gas exiting the calciner and a sufficiently high temperature (close to 950°C) to achieve complete CaO regeneration in short residence times [3, 6–10]. However, oxy-combustion imposes an energy penalty (due to the consumption of fuel and oxygen) and generates additional CO_2 [8, 11–13]. Moreover, the carbonation activity of CaO regenerated at high temperature and under high CO_2 concentration suffers a marked drop, which is particularly intense in the first cycles [10, 14]. Other causes of decay of the sorbent capture capacity are irreversible sulphation due to SO_2 (present in the flue gas and produced in the calciner by oxy-combustion) and losses of fine

particles generated by attrition [3, 15]. It is thus necessary to feed the calciner periodically with a makeup flow of fresh limestone to compensate for sorbent deactivation. As opposed to the sorbent derived from calcination of the initial limestone inventory, CaO derived from the makeup flow is obtained by calcination in a high CO_2 partial pressure environment.

Another naturally occurring mineral that can be used as CaO precursor is dolomite ($CaMg(CO_3)_2$), which is also abundantly available at low price [1, 16, 17]. Arguably, the irreversible decomposition of $MgCO_3$ would enhance the surface area of the calcined sorbent [18], which should favor the CaO reactivity in the fast phase controlled by carbonation on the surface of the solids. Moreover, the presence of MgO in calcined dolomite is expected to increase the thermal stability of the sorbent and help mitigating the loss of CaO carbonation reactivity, which is generally attributed to its superior resistance to sintering at high calcination temperatures. The ultimate mechanism governing the thermal decomposition of dolomite is however not well understood yet [19–21]. The Tamman temperature indicating the initiation of sintering of MgO ($T_t \simeq 1276°C$) [16] is only slightly above the Tamman temperature of CaO ($T_t \simeq 1170°C$) [16] being both values well over the typical calcination temperatures at CaL conditions. Thus, it is unclear why MgO should be resistant to sintering while CaO is not. Furthermore, carbonation of MgO is not thermodynamically favorable at CaL conditions [1, 22]. Hence, the stoichiometric CO_2 capture capacity (ratio of mass of CO_2 chemisorbed to mass of CaO·MgO) of calcined dolomite at CaL conditions is just 0.46 as compared to 0.79 for calcined limestone. Experimental results show accordingly that the capture capacity of dolomite stays well below that of limestone after a certain number of carbonation/calcination cycles [1] even though it must be remarked that most lab-scale tests on dolomite or CaO·MgO synthetic composites do not mimic realistic CaL conditions for postcombustion capture [23–26]. For example, Albrecht et al. [24] observed

that the presence of inert MgO served to increase the conversion of CaO after a very large number of carbonation/calcination cycles (up to 1250). However, these cycles were conducted isothermally at 750°C, subjecting the sample to a 25% CO_2/75% N_2 gas mixture for carbonation during 20 min and calcining it under N_2 during 30 min. A first attempt to compare the multicyclic capture performances of dolomite and limestone when subjected to severe calcination conditions (940°C, 70% vol CO_2) has been recently made [27] by means of a lab-scale bubbling fluidized bed (gas velocities of about 0.5 m/s). Results showed that, despite of its lower Ca content, the sorbent derived from dolomite had a greater capture capacity than limestone derived CaO. However, the sorbents were subjected in this study to only 5 calcination/carbonation cycles in which carbonation was prolonged up to completion and the materials were cooled down to ambient temperature between stages, which is not representative of realistic CaL conditions.

Realistic CaL conditions for postcombustion capture necessarily involve short residence times (of just a few minutes), low CO_2 concentration (about 15% vol) for partial carbonation at around 650°C, high temperature (above 900°C) and high CO_2 concentration (above 70% vol) in the calciner for sorbent regeneration and precalcination of the makeup flow of solids, and very fast transitions between the carbonation and calcination stages (typically of a few seconds) [15, 28]. Moreover, the dual fluidized bed in practice would be operated by rapid gas flows (gas velocities in the range 5 - 10 m/s) in the fast fluidization regime [29] characterized by a high mass/heat transfer efficiency, which is likely impaired in bubbling beds (operated at small gas velocities) wherein gas-solids contacting effectiveness is hindered by the development of gas bubbles [7, 30]. Mass/heat transfer inefficiency may be avoided by means of TGA tests, which however usually fail to reproduce simultaneously the rapid transitions between stages and high CO_2 partial pressure in the calcination environment.

According to process simulations [2, 11, 31, 32] the efficiency of the CaL technology is extraordinarily dependent upon the sorbent capture performance. Thus, it is of paramount importance to characterize it at realistic conditions in order to extract from simulations useful information for the optimum design and operational parameters to scale-up the technology. In the present manuscript we show a comparative study on the multicyclic CO_2 capture behavior of natural dolomite and limestone by means of thermogravimetric analysis (TGA) tests carried out at conditions closely resembling those to be expected in postcombustion capture applications. The role of precalcination conditions and the effect of introducing a recarbonation stage between carbonation and calcination stages will be a particular focus of our study. The incorporation of a recarbonator reactor to the CaL process is thought to improve its efficiency by minimizing the required makeup flow of fresh limestone and the heat demand in the calciner [33–35] albeit in previously reported TGA tests demonstrating the beneficial effect of recarbonation [33, 35, 36] the sorbent was regenerated by calcination in air. More recent works have evidenced that the capture capacity of CaO derived by precalcination of limestone in air and subsequently regenerated by calcination at high temperature/high CO_2 concentration is actually hampered by the introduction of a recarbonation stage [14, 37], which shed doubts on the usefulness of incorporating into the technology an additional recarbonator reactor. As will be seen in this manuscript dolomite and limestone respond in a very distinct way to recarbonation as a function of precalcination conditions. Scanning Electron microscopy (SEM) analysis will be used in our study to gain fundamental knowledge on the mechanisms governing the behavior of both natural CaO precursors.

II. MATERIALS AND METHODS

The materials employed in our work are natural limestone of high purity (99.62% $CaCO_3$, $SiO_2 < 0.05\%$, $Al_2O_3 < 0.05\%$, 0.24% MgO, 0.08% Na_2O) as received from Matagallar quarry (Pedrera, Spain) and a purified natural dolomite ($MgCa(CO_3)_2$) purchased from Alfa Aesar (CAS: 12001-27-3). X-ray diffraction (XRD) patterns measured in our work are shown in Fig. 1. As may be seen, both samples are characterized by a high purity with only a minor presence of $CaCO_3$ impurities in dolomite (as revealed by the small diffraction peak located in the major calcite peak at $2\theta \approx 29.2°$).

The multicyclic CO_2 capture behavior of limestone and dolomite samples has been analyzed by means of carbonation/calcination and carbonation/recarbonation/calcination cycles carried out using a Q5000IR TG analyzer (TA Instruments). This instrument is equipped with a furnace heated by infrared halogen lamps and a high sensitivity balance (<0.1 μg) with a minimum baseline dynamic drift (<10 μg). Infrared heating allows fast and controlled heating/cooling rates (300°C/min) with rather small fluctuations ($< \pm 4$°C). In this way, the transition between the carbonation and calcination stages may be shortened to tens of seconds in contrast with typical TGA tests carried out by using common furnaces with low heating rates (usually below 25°C/min). This is a relevant issue when the sorbent is regenerated under high CO_2 partial pressure since during slow heating it will suffer appreciable recarbonation until the temperature reaches a sufficiently high value (close to 900°C) to reverse the reaction towards decarbonation, which seriously affects its capture performance [14].

Carbonation/calcination (carb/cal) cycles in our TGA tests consisted of 5 min carbonation at 650°C (85% air/15% CO_2 vol/vol) and 5 min calcination at 950°C (70% CO_2/30% air

vol/vol). For comparison, carb/cal tests were also carried out in which calcination was performed at 925°C and 900°C under 70% CO_2/30% air vol/vol, and at 850°C in air. In regards to carbonation/recarbonation/calcination (carb/recarb/cal) cycles, a 3 min recarbonation stage at 800°C (10% air/90% CO_2 vol/vol) was introduced in between the carbonation and calcination stages. TGA tests were initiated by subjecting the samples to different precalcination programs in-situ. On one hand, precalcination was carried out by heating the samples in air at a slow rate (20°C/min) up to 850°C with the goal of replicating the precalcination conditions of the initial solids inventory in the practical application. On the other hand, precalcination was performed by heating up the samples under high CO_2 partial pressure (70% CO_2/30% air vol/vol) up to 950°C (925°C and 900°C in some tests) at a fast rate (300°C/min), which was intended to mimic precalcination of the makeup flow of solids periodically fed into the calciner at practice (due to technical limitations the heating rate was set to 20°C/min from ambient temperature up to 450°C, which is below the reported decomposition temperatures for both materials [23]). The gas flow rate in all the tests was kept small enough (100 cm^3min^{-1}) as to neglect external mass transfer effects. A fixed sample mass of 10 mg was employed in all the runs, which allows dismissing also any effect of diffusion resistance through the sample on the reaction rate [38]. Particle size in our samples was below 500 μm, thus intra-particle diffusion resistance can be disregarded too [39, 40]. TGA tests were complemented with microscopy analysis of the cycled samples by means of a ultra high-resolution Scanning Electron Microscope (SEM HITACHI S5200).

III. EXPERIMENTAL RESULTS AND DISCUSSION

A. CO_2 capture capacity

In order to take into account the presence of inert MgO in the sorbent derived from dolomite, the appropriate parameter for practical purposes to characterize the sorbent performance is the capture capacity, which is defined as the ratio of mass of CO_2 captured to the mass of sorbent before each carbonation stage (including both CaO and MgO in the case of dolomite). Figure 2 shows multicyclic capture capacity results from carb/cal tests in which dolomite and limestone samples were precalcined in air and regenerated either in air at 850°C (Fig. 2a) or under 70%CO_2 at 950°C (Fig. 2b), respectively. As might be expected, dolomite exhibits a lower capture capacity during the first cycles after precalcination in air but it deactivates with the cycle number at a lower rate as compared with limestone. Under these conditions (sorbent regeneration in air, Fig. 2a) limestone deactivation is not marked and both sorbents exhibit a similar performance after the 5th carb/cal cycle. However, the scenario is radically changed when the sorbents are regenerated under realistic (postcombustion capture) calcination conditions (Fig. 2b). In this case, limestone suffers a drastic drop of its capture capacity after regeneration and it falls below 0.05 in just 10 cycles. In contrast, dolomite deactivates at a much lower rate. As a result, the capture capacity of dolomite is twice that of limestone after 20 cycles.

The effect of recarbonation on the performance of both sorbents precalcined in air and regenerated under high CO_2 concentration is illustrated by Figs. 3a and 3b. As can be seen, recarbonation is actually detrimental for the carbonation activity of limestone cycled under these conditions. Conversely, recarbonation does not cause an appreciable effect on the performance of dolomite. Likewise, the behavior of dolomite is not essentially changed

by the conditions of precalcination as seen in Fig. 4 where capture capacity data are plotted from carb/calc tests in which precalcination was carried out either in air at 850°C or under 70%CO_2 at 950°C. Contrarily, precalcination conditions play a relevant role on the multicyclic behavior of limestone (see Fig. 4). Severe precalcination conditions cause a significant drop of the capture capacity of limestone derived CaO in the 1st cycle but it serves to mitigate its progressive decay with the number of cycles. After 20 cycles, the capture capacity of the limestone sample precalcined under high CO_2 concentration is about 0.08 as compared to just 0.04 when limestone was precalcined in air. Still dolomite exhibits a neatly higher capture capacity also when precalcination conditions are severe (see Fig. 5). Figure 6 shows the effect of recarbonation on the performance of the sorbents precalcined and regenerated under severe conditions. Interestingly, recarbonation has in this case a favorable influence on the performance of limestone whereas the behavior of dolomite remains quite insensitive to recarbonation up to the 10th cycle after which the capture capacity of the sorbent subjected to recarbonation becomes only slightly hindered.

As a summary, TGA results demonstrate that dolomite exhibits a multicyclic capture capacity which does not suffer remarkable variations with either sorbent recarbonation or the conditions of precalcination. Conversely, the behavior of limestone is highly dependent on both. Only if limestone is precalcined under severe conditions involving high CO_2 concentration (similar to those of regeneration) and is subjected to an intermediate recarbonation stage, its capture capacity may keep the pace with that of dolomite subjected to ordinary carb/calc cycles as seen in Fig. 7. From the point of view of sorbent capture performance at realistic CaL conditions, these results suggest that the use of natural dolomite for post-combustion capture would yield an efficiency improvement of the CaL technology, which is comparable to that of introducing a recarbonator reactor when using limestone (with the

added requirement, if limestone is employed, of precalcining under high CO_2 partial pressure instead of air in order to avoid marked deactivation as seen in our work). An additional gain of efficiency may be achieved by the possibility of calcining at lower temperatures. This relevant issue will be discussed in detail in section IV. In regards to the sorbent behavior, it is interesting to remark that the capture capacity of dolomite is practically insensitive to the temperature of precalcination/regeneration in the range of temperatures between 900°C and 950°C as seen in Fig. 7, which stresses further the main role of MgO on avoiding sintering and deactivation of CaO at high temperatures.

B. CaO conversion

Let us recall that, for practical purposes, the parameter used above to compare the multicyclic CO_2 capture performances of dolomite and limestone has been the capture capacity. From a fundamental perspective it is also interesting to look at the CaO conversion defined as the ratio of mass of CaO converted in each carbonation stage to the mass of CaO initially present in the sorbent after calcination. In the case of limestone, CaO conversion is readily obtained multiplying the capture capacity by the factor M_{CaO}/M_{CO2} where $M_{CaO} = 56$ g/mol and $M_{CO2} = 44$ g/mol are the molecular weights of CaO and CO_2, respectively. For dolomite, the sorbent derived after calcination consists of MgO·CaO. CaO conversion is then obtained multiplying the capture capacity by the factor $(1+M_{MgO}/M_{CaO})M_{CaO}/M_{CO2}$ where $M_{MgO} = 40$ g/mol is the molecular weight of MgO. Figure 8 shows data on multicyclic CaO conversion for both sorbents precalcined either in air (at 850°C) or under 70%CO_2 (at 950°C) and regenerated under severe conditions (note the log-log scale). Multicyclic CaO conversion data reported in the literature is usually fitted by the semi-empirical equation [41–43]

$$X_N = X_r + \frac{X_1}{k(N-1) + (1 - X_r/X_1)^{-1}}; \qquad (N = 1, 2...) \tag{1}$$

where N is the cycle number, X_1 is CaO conversion at the 1st cycle, k is a deactivation constant and X_r is the so-called residual conversion, which is asymptomatically approached for a very large number of cycles. Most of TGA data obtained for natural limestones can be reasonably well fitted using Eq. 1 with a residual conversion between 0.07 and 0.08 and a deactivation constant k around 0.5 [41, 44]. Usually, process simulations and economic analysis on the CaL technology rely on these values to characterize the sorbent behavior [2, 12, 31, 33, 34, 45]. Yet, most lab-scale tests are not carried out under realistic (post-combustion capture) calcination conditions due to technical limitations as explained above. As may be seen in Fig. 8, CaO conversion data obtained in our work for limestone precalcined and regenerated under high CO_2 concentration still converges towards a residual value ($X_r = 0.079$), which fits within the interval commonly reported for limestones precalcined and regenerated under low CO_2 concentration even though the deactivation constant obtained from our data is substantially higher ($k = 0.85$). In regards to the multicyclic CaO conversion of limestone precalcined in air and regenerated under high CO_2 concentration, in the first 10 cycles it follows a trend marked by a drastic drop which cannot be satisfactorily fitted by Eq. 1 (see Fig. 8). Under these conditions, Eq. 1 conforms well to the evolution of CaO conversion data only from the 10th cycle yielding a residual value of just $X_r = 0.034$. On the other hand, the behavior of CaO conversion for dolomite does not exhibit such a critical dependence on precalcination conditions and reaches a quite high residual value as compared to limestone. Note that, even after precalcination under severe conditions, CaO conversion for dolomite in the 1st cycle is about $X_1 = 0.794$ whereas for limestone it falls down to just $X_1 = 0.476$

C. SEM analysis

Our TGA results indicate that the CaO skeleton derived from precalcining limestone in air is highly reactive, yet when the sorbent is regenerated under high CO_2 concentration/high temperature (a must for postcombustion capture) it suffers a drastic deactivation which is additionally intensified by recarbonation. SEM pictures of limestone and dolomite samples precalcined in air and subjected to carb/calc cycles under severe regeneration conditions are shown in Fig. 9. Clearly, limestone derived CaO appears as markedly sintered. The consequent reduction of its reactive surface area is in accordance with the significant drop of the fast carbonation activity obtained from the TGA tests (Fig. 4a). On the other hand, the cycled dolomite sample exhibits a much higher porosity. As inferred from TEM (in-situ) and XRD analysis reported elsewhere [21] on dolomite crystals calcined at temperatures in the range 500–1000°C, decomposition of dolomite occurs by de-mixing of a metastable CaO·MgO precursor and the subsequent formation of pure CaO and MgO crystals via oriented aggregation and sintering, which is favored by high ion diffusivity, although it must be noticed that calcination in those tests was carried out in air and vacuum (we will come back to this argument in section IV). In our SEM pictures, individual MgO grains segregated from sintered CaO can be clearly identified (Fig. 9). MgO grains have a regular size of around 100nm and appear to be rather resistant to sintering. In fact, these SEM images of cycled dolomite samples show a striking resemblance with SEM images shown in our previous work [46] of a CaO-based sorbent synthesized by impregnation of a calcium nitrate solution on a nanostructured calcium silicate matrix (see Fig. 10), which acted as a thermally stable support for CaO. Similarly, it may be argued that the thermal stability and enhanced porosity provided by the nanostructured MgO skeleton in the case of cal-

cined dolomite allows the capture capacity of the dolomite derived sorbent to outweigh the performance of limestone derived CaO, which is critically impaired when regenerated by calcination under severe realistic conditions.

In some of the SEM images obtained in our work there is a marked segregation between the MgO nanostructured grains and the sintered CaO skeleton. This is particularly noticeable in the case of dolomite samples subjected to carb/recarb/carb cycles (precalcined and regenerated under severe conditions) as may be seen in Fig. 11. Since diffusivity is enhanced under the conditions of recarbonation (high temperature and high CO_2 concentration) [47–49], it is likely that the segregation of MgO and CaO grains is promoted in accordance with the mechanism reported elsewhere form in-situ observations [21]. This would lead to a loss of efficiency of the MgO skeleton on enhancing the sorbent capture capacity, which can be the reason for the observed slight decline of capture capacity performance of the dolomite sample precalcined under severe conditions and subjected to a recarbonation stage (Fig. 6b). SEM pictures of cycled limestone and dolomite samples under diverse conditions can be seen in Fig. 12 and show in general a higher porosity of the CaO skeleton for dolomite in accordance with the higher conversion exhibited by this sorbent. Remarkably, MgO grains are not visible in the surface of the cycled dolomite samples shown in Fig. 12. Figure 13 illustrate more clearly this phenomenon usually observed in the SEM pictures. Presumably, repeated carbonation/calcinations on the surface of the particles and significant sintering of the nascent CaO grains supported on the inert MgO skeleton would be responsible for this segregation. As may be seen in these pictures, MgO grains have a tendency to migrate towards the interior of the particles whereas sintered CaO grains build up onto the surface of the particles. This kind of segregation is clearly observed in the representative photographs on the right of Fig. 13, where the cross section of a fractured particle is featured.

IV. KINETICS OF LIMESTONE AND DOLOMITE CALCINATION

Simulations of the CaL technology at the industrial level show that the energy demand in the calciner can reach a fraction near half the total energy required in the process [11] or even higher if the detrimental effect on limestone performance caused by regeneration under high CO_2% were taken into account. Many research efforts are thus currently devoted to the development of innovative techniques to achieve a high calciner efficiency at a decreased temperature and taking into account the short residence times imposed [15, 28]. Our goal in this section is to carry out a comparative analysis of the decarbonation kinetics of limestone and dolomite during calcination in our TGA tests.

As seen in Fig. 14 limestone and dolomite follow very similar decarbonation kinetics when calcined in air by slowly increasing the temperature up to 850°C. In agreement with observations reported in the literature [50, 51], we see that decarbonation of dolomite in air occurs in one stage and starts at about 600°C analogously to limestone. Figure 15 illustrates the kinetics of limestone calcination under 70%CO_2 by quickly increasing the temperature up to 950°C. As may be seen, the presence of CO_2 hinders severely decarbonation of limestone as widely reported in the literature [39, 52–58]. Since $CaCO_3$ decarbonation is heavily influenced by the thermodynamic equilibrium the presence of CO_2 displaces it to higher temperatures but also slows down it markedly. Decarbonation is seen to start in Fig. 15 at about 900°C (around 30°C above the thermodynamic equilibrium temperature under 70%CO_2 at atmospheric pressure [39]) and only progresses at a sufficiently fast rate to be fully attained in a short residence time if the calcination temperature is raised above 925°C in accordance with pilot-scale tests results [3, 7–10]. As compared to limestone, the kinetics of dolomite calcination under 70%CO_2 shows radically different features as

may be observed in Fig. 16. In agreement with previous works [50, 51], decomposition of dolomite under high CO_2 concentration is seen to occur mainly by two stages. Irreversible $MgCO_3$ decomposition occurs in a first stage whereas the second stage involving $CaCO_3$ decomposition is initiated at around 650°C, which is well below the equilibrium temperature for pure $CaCO_3$ decomposition. As shown in Fig. 16, decarbonation of dolomite is fully achieved in a time period below 5 minutes at a calcination temperature of just 900°C.

The thermal decomposition of dolomite via a single step at low partial pressures of CO_2 and along two distinct stages at high CO_2 partial pressures observed in our work is a well documented phenomenon, yet the mechanism responsible for this behavior is still a subject of debate [19–21, 23, 51, 59–61]. Experimental studies have shown that the intermediate products between stages in the decomposition process under CO_2 are $MgCO_3$, $CaCO_3$ and MgO while the final products were CaO and MgO. Thus, it is usual to represent the process by means of the reactions

$$CaMg(CO_3)_2 \rightarrow CaCO_3 + MgO + CO_2$$

$$CaCO_3 \rightarrow CaO + CO_2$$

De-mixing of Ca^{2+} and Mg^{2+} cations in the 1st stage (half-decomposition) is thought to yield the nucleation and growth of MgO crystals resistant to sintering and the concomitant formation of $CaCO_3$ through the diffusion of its constituents within the lattice. Solid-state diffusion (of cations in the lattice and of CO_3^{2-} across the reacting interface) are thus believed to be the rate-limiting factors of half-decomposition. As a matter of fact, it is reported that the half-decomposition temperature is considerably decreased by grinding the dolomite sample [51], which is known to decrease the resistance to solid-state diffusion

[48, 49]. An alternative more compact representation of the reaction is [59]

$$CaMg(CO_3)_2 \rightarrow CaCO_3 + MgCO_3$$

being $MgCO_3$ thermodynamically unstable at relatively lower temperatures [23], which gives rise to the two-stage decomposition process. In accordance with this formulation we see that the 1st weight loss (Fig. 16) occurs within the temperature range 400–500°C, which conforms to the equilibrium temperature of $MgCO_3$ decomposition at a CO_2 partial pressure of 0.7 atm [23] (70% vol concentration at atmospheric pressure in our tests). Nonetheless, half-decomposition is generally observed at higher temperatures [60] in experiments usually carried out at low heating rates ($\sim$ 10°C/min). In our tests, 1st chemical decomposition is triggered just when the heating rate is increased to 300°C/min, which suggests that the heating rate plays a relevant role on the mechanism of the process. On the other hand, Fig. 16 shows that $MgO{\cdot}CaCO_3$ decomposition would be started at temperatures well below the equilibrium temperature for pure $CaCO_3$ decomposition ($T_{eq} \approx 870$°C) whereas the kinetics of $MgO{\cdot}CaCO_3$ decomposition would be significantly enhanced as compared to limestone decomposition under CO_2.

Figure 17 illustrates the kinetics of $CaCO_3$ and $MgO{\cdot}CaCO_3$ decomposition during CaO regeneration in the 1st carb/calc cycle. As opposed to the contrasting behaviors exhibited by limestone and dolomite calcination, it is observed that the calcination kinetics for both sorbents is similar in this regeneration stage under high CO_2 concentration. Decarbonation commences at about 850°C and proceeds at a quick rate, which is still faster for the dolomite derived sorbent. Arguably, desorption of CO_2 at high CO_2 partial pressure would be favored across the boundaries between different phases. The $CaCO_3$/CaO transformation experi-

enced by both sorbents during regeneration would be thus governed by a similar mechanism with the MgO grains serving as a stable nano-structured support for the dolomite derived CaO and favoring solid-state diffusion.

V. CAO REGENERATION AND SINTERING

The loss of multicyclic CaO conversion is usually explained from the marked sintering suffered by the CaO skeleton regenerated by calcination at high temperature [41, 43]. The point at which sintering begins in ceramic materials occurs at the Tammann temperature, which, as a rule of thumb, is considered as half their melting temperature. As seen in our SEM pictures, CaO grains of dolomite samples subjected to repeated carb/cal cycles exhibit indeed notable sintering, yet MgO grains appear resistant to sintering. This is a puzzling observation if one takes into account that the Tammann temperatures of both oxides are not very different ($T_t \simeq 1170$°C for CaO and $T_t \simeq 1276$°C for MgO) [16] and both are well over the calcination temperature at CaL conditions. However, the main reason for the sintering dissimilarity of both oxides must be sought in their different multicyclic history. The essential issue is that CaO undergoes repeated carbonation and regenerations whereas MgO remains as an inert oxide. It may be therefore hypothesized that most of CaO sintering occurs during the $CaCO_3$/CaO transformation in each cycle. Figure 18 shows limestone derived CaO conversion data from carb/calc cycles in which the calcination stages were prolonged to 3 hours. As may be seen, and despite the excessively long calcination periods, CaO conversion is not remarkably decreased as compared to conversion in the tests with short calcination stages (5 min) mimicking practical conditions, which supports the argument that sintering and deactivation occurs mostly in the nascent CaO during the $CaCO_3$/CaO transformation and not after CaO has reached its stable form.

Empirical measurements reported in a wide number of works indicate that the sintering of CaO is greatly accelerated when CO_2 is present in the calcination atmosphere at high concentration [42, 57, 62] whereas the $CaCO_3$ decarbonation rate suffers a drastic decline [39, 52–58]. Gaining understanding on the physicochemical mechanism behind this behavior should be a main scientific focus of studies on the CaL process since it determines the multicyclic sorbent performance and therefore has a great influence on the efficiency of the technology. Decarbonation of $CaCO_3$ is initiated by the chemical decomposition of $CaCO_3$ to yield CaO and CO_2 adsorbed, which is afterwards desorbed [39, 52]. At low CO_2 partial pressures, the process is rate limited by the chemical decomposition stage since desorption is very fast [39]. In the case of high CO_2 partial pressure however, CO_2 desorption is severely hampered and would limit the decarbonation process [56]. Empirical studies indicate that the presence of CO_2 at high concentrations in the calcination atmosphere leads to a reversible CO_2 desorption/adsorption dynamic process [53, 56] that would slow down decarbonation. In the pioneer work of Hyatt et al. [52], experimental measurements on the rate of calcite crystals calcination lead the authors to formulate the hypothesis that the nascent CaO lattice acquires a metastable rhombohedral structure (similar to the original $CaCO_3$) when CO_2 is desorbed, after which the stable CaO cubic lattice nucleates from the transformation of the metastable CaO, which acts as bridge for the reaction. Later results from XRD analysis upheld the idea that a distorted metastable phase of CaO was formed during decarbonation of calcite [63, 64] although little could be concluded about its crystal structure. A more recent study [65] has shown from diverse advanced characterization techniques that the $CaCO_3$/CaO transformation starts by the formation of a mesoporous structure made up of rod-shaped (metastable) CaO nanocrystals on each rhombohedral cleavage face of the calcite pseudomorph. These CaO nanocrystals undergo oriented aggregation driven by van der

Waals attractive forces to minimize surface energy. Aggregated nanocrystals become afterwards sintered as decomposition progresses. Oriented aggregation and sintering reduces the surface area and porosity of the metastable structure by closing the mesopores between the rod-shaped CaO nanocrystals, which results in the formation of macropores through which CO_2 can easily escape to complete the transformation by the nucleation of stable CaO cubic crystals [65]. Chemical decomposition was observed to control the kinetics of the process during most of the $CaCO_3$/CaO transformation in these experiments [65], which were carried out in vacuum and air. Under these conditions there is no significant resistance against CO_2 diffusion to migrate outside the metastable CaO structure. However, the resistance for CO_2 to escape the metastable CaO mesoporous structure by diffusion would be impaired under a high CO_2 partial pressure in the environment outside the solid, which would favor re-adsorption of CO_2. It is well known that adsorption of CO_2 on solid surfaces gives rise to a significant increase of the surface energy and therefore enhances the attractive force between the solids [66]. Thus, it may be expected that, in the presence of CO_2 adsorbed onto the surfaces of metastable CaO nanocrystals, their aggregation is promoted, which would favor their subsequent sintering. In regards to decarbonation during regeneration of MgO·$CaCO_3$, it may be argued that the presence of inert MgO nanocrystals between the CaO metastable nanocrystals would reduce their attractive forces, thus counteracting the effect of high CO_2 partial pressure by preventing their adhesive aggregation and subsequent sintering. As the number of cycles progresses, the cumulative aggregation and sintering of CaO nanocrystals in each $CaCO_3$/CaO transformation would lead to a segregation between the sintered CaO skeleton and the resistant to sintering MgO grains as observed from our SEM analysis. Moreover, this argument may explain why sintered CaO is mostly seen on the surface of cycled dolomite particles since it is there where most of CaO carbonation/regeneration takes

place in short residence times. Further research must be devoted in future works to explore the fundamental mechanism of $CaCO_3$/CaO transformation at high CO_2 pressure but it seems clear that the multicyclic loss of CaO conversion when subjected to repeated carb/cal cycles is determined by the evolution of metastable CaO formed during the $CaCO_3$/CaO transformation in each regeneration stage. From the practical point of view, it would be interesting to devise feasible strategies to tailor this transformation by minimizing aggregation and sintering of metastable CaO nanocrystals. Presumably, this is the role played by the MgO inert grains in natural dolomite.

VI. INFLUENCE OF SORBENT PERFORMANCE ON THE CAL TECHNOLOGY EFFICIENCY

Leaving aside the question on the fundamental mechanism that governs limestone and dolomite decompositions under high CO_2 concentration, our results suggest that the use of dolomite in the CaL technology would allow decreasing the temperature of the calciner significantly. In regards to limestone, process simulations [8] show that the minimum calcination temperature to achieve an acceptable calciner efficiency would be above 930°C whereas the calciner efficiency would be severely hampered if the temperature is decreased to 900°C, which agrees with our observations on the kinetics of limestone decarbonation under high CO_2 concentration. On the other hand, our results indicate that a sufficiently high calciner efficiency would be attainable at 900°C if natural dolomite is used, which decomposes quickly at this reduced temperature under a high CO_2 concentration environment. According to process simulation results [11] a decrease of the calcination temperature from 950°C to 900°C (while maintaining a high calciner efficiency) may bring about a substantial reduction of costs. Particularly, the amounts of coal and oxygen needed for oxy-combustion

to raise the calciner temperature and the additional CO_2 produced by oxy-combustion, which represent an important penalty for the technology [13, 28], would be lowered. Process simulations [13, 45] indicate that the ratio of the mass of coal needed for oxy-combustion to the mass of CO_2 captured would be decreased by a 10% if the calciner temperature is decreased from 950°C to 900°C in the ordinary CaL configuration. If limestone is used, the calciner temperature should be kept at 950°C and a similar 10% reduction would be possible by incorporating a cyclonic preheater to transfer heat from hot gas leaving the calciner to the solids coming out from the carbonator, which has been proposed as a feasible innovation to improve the industrial competitiveness of the technology [13]. Process simulations indicate also that a low calciner to carbonator inventory ratio (of about 0.2) would be only possible for limestone by calcining at 950°C (which yields a high calciner efficiency) whereas a decrease of the calciner temperature to 900∘C would require increasing this ratio to about 1.2 [13]. Since full decarbonation at realistic CaL conditions could be efficiently attained at 900°C for dolomite, it may be expected that the use of dolomite would allow for a considerable reduction of the solids inventory in the calciner further decreasing the energy penalty of the technology. Process simulations also show that the CaO/CO_2 molar ratio (R) can be substantially decreased by a decrease of the calcination temperature for a constant purge flow of solids (f) and if the capture efficiency (η) is kept constant as would be possible by using dolomite. For example, for $f = 3\%$ and $\eta = 0.85$, it would be $R \simeq 10$ at 950°C and $R \simeq 7.5$ at 900°C [13]. The amount of solids purge and make-up flows have a relevant influence on the process performance [12, 31]. Large purge flows lead to a dramatic increase of the heat demand for calcination and hence the cost for oxygen production and auxiliaries consumption is raised. Thus, the cost of CO_2 avoided tonne (tCO_2) is minimized at relatively low purges. At an optimum CaO/CO_2 molar ratio of $R = 5$ and only $f = 1\%$

purge the estimated cost is around 14/tCO_2 whereas an increase of the purge flow in the calciner (as would be required by enhanced deactivation) to 2.5% would increase the tCO_2 avoided cost by $\sim$1 /tCO_2 [31].

An additional important aspect to be carefully addressed in future TGA studies on limestone and dolomite at realistic CaL conditions is the irreversible sulphation of the sorbent due to the presence of SO_2 either in the flue gas in the carbonator or in the calciner due to oxy-combustion, which causes a notable decay of CaO conversion [10, 27, 67]. The main factor limiting CaO sulphation reactivity is pore blocking [68–70]. Sulphation is essentially favored by sintering and hence sulphation conversion is observed to increase with the cycle number in multicyclic carb/cal tests [9]. Since CaO sintering is mitigated in the dolomite derived sorbent, sulphation would be presumably minimized by the use of dolomite as compared to limestone. Moreover, the possibility of lowering down the calciner temperature would allow decreasing the generation of SO_2 in this reactor, which would serve to further mitigate deactivation of the sorbent as caused by sulphation thus allowing for a reduction of the makeup of fresh solids to counterbalance the purge flow of the solids deactivated. Moreover, as seen in our work (Fig. 2b), the capture capacity of dolomite is substantially higher than that of limestone for the initial solids inventory precalcined in air, which would allow further decreasing the amount of purged solids while the capture efficiency is kept at a high level [31]. On the other hand, our results show (section III A) that, for the solids precalcined under high CO_2 concentration, the multicyclic capture behavior of dolomite in ordinary carb/calc cycles is similar to that of limestone when an intermediate recarbonation stage is introduced with the goal of reducing the amount of purged solids to a minimum required for desulfurization as proposed elsewhere [33–35]. Simulations of a large-scale system indicate that a bubbling recarbonator reactor with a cross-sectional area of between 80

and 100 m^2, expanded bed height of 2 m, and inlet gas velocities of 0.6 - 0.9 m/s would be needed for this purpose [71]. According to simulations, by introducing a recarbonatior reactor, the make-up flow of limestone would be as low as 0.07 kg limestone per kg coal as compared to 0.35 kg limestone per kg coal predicted in the ordinary CaL configuration [33], which would lead to a significant reduction in energy consumption and coal/oxygen for oxy-combustion (albeit it must be reminded that these simulations were based on the assumption of a sorbent behavior inferred from TGA tests in which the samples were regenerated under low CO_2 concentration [33, 35]). Since, as observed in our work, the performance of dolomite subjected to ordinary carb/calc cycle is similar to that of limestone subjected to carb/recarb/calc cycles, the reduction of costs by using dolomite instead of limestone could be estimated from the costs involving the incorporation of an additional recarbonator reactor to reactivate the limestone derived CaO, which should be re-assessed by considering the sorbents behavior under realistic regeneration conditions. A potential issue related to the use of dolomite in the CaL technology is its friability as suggested in some works [27], which may be due to the development of intense residual stresses inside the porous matrix of the solid during decomposition [19] also leading to decrepitation phenomena observed in TGA tests [59, 72]. Particle fragmentation would occur however only during dolomite decomposition and not in the sorbent regeneration stage. Accordingly, the rate of generation of fine particle fragments in lab-scale fluidized bed tests [27] has been observed to be significant just in the first calcination.

VII. CONCLUSIONS

A main conclusion of our study is that natural dolomite can be an advantageous alternative to limestone as sorbent precursor for postcombustion CO_2 capture by means of the CaL

technology. TGA tests carried out under realistic sorbent regeneration conditions (high CO_2 concentration, high temperature and quick transitions between carbonation and calcination stages) show that the capture capacity of limestone derived CaO is critically influenced by precalcination conditions and an intermediate recarbonation stage. The capture capacity of CaO derived from precalcining limestone in air suffers a drastic drop in the first cycles. Moreover, the introduction of a recarbonation stage, which is intended in practice to minimize the need for a makeup flow of fresh limestone fed to the calciner, would actually have an adverse effect on the capture capacity of the sorbent derived from precalcining the initial inventory of limestone in air. SEM analysis of CaO derived from limestone precalcined in air and regenerated under high CO_2 concentration/high temperature show that it suffers marked sintering. The multicyclic stability of CaO may be enhanced if precalcination is carried out under the same conditions as those used for regeneration, which leads also to a favorable effect of recarbonation. On the other hand, the behavior of the sorbent derived from dolomite is quite insensitive to either precalcination or recarbonation conditions and shows a neatly higher capture capacity as compared to limestone at realistic calcination conditions. The predictability of dolomite behavior, regardless of precalcination and recarbonation conditions, can be a further advantage over the strong dependence of limestone performance on these conditions, which may vary uncontrollably in any modification of the process. For example, proposed innovations of the CaL technology such as the addition of a cyclonic preheater to transfer heat from the hot gas leaving the calciner to the particles exiting the carbonator [13] will lead to recarbonation of the partially carbonated solids. In this case, and if the makeup flow of fresh limestone fed to the calciner is minimized, the activity of the sorbent precalcined in air might be further hindered. SEM analysis demonstrates that, after a number of carbonation/calcination cycles, MgO and CaO grains in

the dolomite samples become segregated with resistant to sintering MgO grains migrating towards the interior of the particles and a CaO layer building up on their surface. The improved stability provided by the inert MgO skeleton would serve to significantly enhance the multicyclic CaO conversion and sorbent capture capacity at realistic CaL conditions for postcombustion CO_2 capture. An additional potential advantage brought about by the use of dolomite would be its much faster decomposition under CO_2 as compared to limestone, which would allow reducing notably the temperature of the calciner that imposes the main energy penalty to the technology.

VIII. ACKNOWLEDGEMENTS

This work was supported by the Andalusian Regional Government Junta de Andalucia (contracts FQM-5735, TEP-7858 and TEP-1900), Spanish Government Agency Ministerio de Economia y Competitividad and FEDER funds (contracts FIS2011-25161 and CTQ2011-27626). One of the authors (PESJ) is supported by the Juan de la Cierva program of the Spanish Ministerio de Economia y Competitividad. We gratefully acknowledge the XRD and SEM services of the Innovation, Technology and Research Center of the University of Seville (CITIUS). The valuable assistance of Dr. Francisco Varela (CITIUS) with the microscopy analysis and fruitful discussions with Drs. Luis M Romeo and Pilar Lisbona (University of Zaragoza-CIRCE) are warmly appreciated.

IX. REFERENCES

[1] J. Blamey, E. J. Anthony, J. Wang, and P. S. Fennell, "The calcium looping cycle for large-scale CO_2 capture," *Prog. Energ. Combust. Sci.*, vol. 36, no. 2, pp. 260–279, 2010.

[2] M. C. Romano, "Modeling the carbonator of a Ca-looping process for CO_2 capture from power plant flue gas," *Chemical Engineering Science*, vol. 69, pp. 257 – 269, 2012.

[3] B. Arias, M. Diego, J. Abanades, M. Lorenzo, L. Diaz, D. Martinez, J. Alvarez, and A. Sanchez-Biezma, "Demonstration of steady state CO_2 capture in a 1.7 MWth calcium looping pilot," *International Journal of Greenhouse Gas Control*, vol. 18, pp. 237–245, 2013.

[4] M. C. Romano, I. Martinez, R. Murillo, B. Arstad, R. Blom, D. C. Ozcan, H. Ahn, and S. Brandani, "Process simulation of Ca-looping processes: review and guidelines," *Energy Procedia*, vol. 37, pp. 142 – 150, 2013.

[5] M.-H. Chang, C.-M. Huang, W.-H. Liu, W.-C. Chen, J.-Y. Cheng, W. Chen, T.-W. Wen, S. Ouyang, C.-H. Shen, and H.-W. Hsu, "Design and experimental investigation of Calcium Looping process for 3-kWth and 1.9-MWth facilities," *Chemical Engineering & Technology*, vol. 36, no. 9, pp. 1525–1532, 2013.

[6] J. Ströhle, M. Junk, J. Kremer, A. Galloy, and B. Epple, "Carbonate looping experiments in a 1MWth pilot plant and model validation," *Fuel*, vol. 127, no. 0, pp. 13 – 22, 2014. Fluidized Bed Combustion and Gasification CO2 and SO2 capture: Special Issue in Honor of Professor E.J. (Ben) Anthony.

[7] A. Charitos, N. Rodriguez, C. Hawthorne, M. Alonso, M. Zieba, B. Arias, G. Kopanakis, G. Scheffknecht, and J. C. Abanades, "Experimental validation of the Calcium Looping CO_2

capture process with two circulating fluidized bed carbonator reactors," *Industrial & Engineering Chemistry Research*, vol. 50, no. 16, pp. 9685–9695, 2011.

[8] I. Martinez, G. Grasa, R. Murillo, B. Arias, and J. Abanades, "Modelling the continuous calcination of $CaCO_3$ in a Ca-looping system," *Chemical Engineering Journal*, vol. 215–216, pp. 174–181, 2013.

[9] R. T. Symonds, D. Y. Lu, V. Manovic, and E. J. Anthony, "Pilot-scale study of CO_2 capture by cao-based sorbents in the presence of steam and SO_2," *Industrial & Engineering Chemistry Research*, vol. 51, no. 21, pp. 7177 – 7184, 2012.

[10] A. Coppola, F. Scala, P. Salatino, and F. Montagnaro, "Fluidized bed calcium looping cycles for CO_2 capture under oxy-firing calcination conditions: Part 1. assessment of six limestones," *Chemical Engineering Journal*, vol. 231, pp. 537 – 543, 2013.

[11] N. Rodriguez, M. Alonso, G. Grasa, and J. C. Abanades, "Heat requirements in a calciner of $CaCO_3$ integrated in a CO_2 capture system using CaO," *Chemical Engineering Journal*, vol. 138, no. 1–3, pp. 148–154, 2008.

[12] L. M. Romeo, Y. Lara, P. Lisbona, and J. M. Escosa, "Optimizing make-up flow in a CO_2 capture system using CaO," *Chemical Engineering Journal*, vol. 147, no. 2-3, pp. 252 – 258, 2009.

[13] A. Martinez, Y. Lara, P. Lisbona, and L. M. Romeo, "Operation of a cyclonic preheater in the Ca-looping for CO_2 capture," *Environmental Science & Technology*, vol. 47, no. 19, pp. 11335–11341, 2013.

[14] J. M. Valverde, P. E. Sanchez-Jimenez, and L. A. Perez-Maqueda, "Calcium-looping for post-combustion CO_2 capture. on the adverse effect of sorbent regeneration under CO_2," *Applied Energy*, vol. 126, pp. 161–171, 2014.

[15] J. Ylatalo, J. Ritvanen, T. Tynjala, and T. Hyppanen, "Model based scale-up study of the calcium looping process," *Fuel*, vol. 115, pp. 329–337, 2014.

[16] A. M. Kierzkowska, R. Pacciani, and C. R. Müller, "CaO-based CO_2 sorbents: From fundamentals to the development of new, highly effective materials," *ChemSusChem*, vol. 6, no. 7, pp. 1130–1148, 2013.

[17] J. M. Valverde, "Ca-based synthetic materials with enhanced CO_2 capture efficiency," *J. Mater. Chem. A.*, vol. 1, p. 447 468, 2013.

[18] J. E. Readman and R. Blom, "The use of in situ powder X-ray diffraction in the investigation of dolomite as a potential reversible high-temperature CO_2 sorbent," *Phys. Chem. Chem. Phys.*, vol. 7, pp. 1214–1219, 2005.

[19] D. Beruto, R. Vecchiattini, and M. Giordani, "Effect of mixtures of H_2O (g) and CO_2 (g) on the thermal half decomposition of dolomite natural stone in high CO_2 pressure regime," *Thermochimica Acta*, vol. 404, no. 1–2, pp. 25–33, 2003.

[20] H. Galai, M. Pijolat, K. Nahdi, and M. Trabelsi-Ayadi, "Mechanism of growth of MgO and $CaCO_3$ during a dolomite partial decomposition," *Solid State Ionics*, vol. 178, no. 15–18, pp. 1039 – 1047, 2007.

[21] C. Rodriguez-Navarro, K. Kudlacz, and E.Ruiz-Agudo, "The mechanism of thermal decomposition of dolomite: New insights from 2D-XRD and TEM analyses," *American Mineralogist*, vol. 97, pp. 38–51, 2012.

[22] K. Chrissafis, C. Dagounaki, and K. Paraskevopoulos, "The effects of procedural variables on the maximum capture efficiency of CO_2 using a carbonation/calcination cycle of carbonate rocks," *Thermochimica Acta*, vol. 428, no. 12, pp. 193 – 198, 2005.

[23] A. Silaban, M. Narcida, and D. P. Harrison, "Characteristics of the reversible reaction between CO_2(g) and calcined dolomite," *Chemical Engineering Communications*, vol. 146, no. 1, pp. 149–162, 1996.

[24] K. O. Albrecht, K. S. Wagenbach, J. A. Satrio, B. H. Shanks, and T. D. Wheelock, "Development of a CaO-based CO_2 sorbent with improved cyclic stability," *Ind. Eng. Chem. Res.*, vol. 47, p. 7841 7848, 2008.

[25] D. S. Sultan, C. R. Muller, and J. S. Dennis, "Capture of CO_2 using sorbents of calcium magnesium acetate (CMA)," *Energy & Fuels*, vol. 24, no. 6, pp. 3687–3697, 2010.

[26] X. Yang, L. Zhao, S. Yang, and Y. Xiao, "Investigation of natural CaO-MgO sorbent for CO_2 capture," *Asia-Pacific Journal of Chemical Engineering*, vol. 8, no. 6, pp. 906–915, 2013.

[27] A. Coppola, F. Scala, P. Salatino, and F. Montagnaro, "Fluidized bed calcium looping cycles for CO_2 capture under oxy-firing calcination conditions: Part 2. assessment of dolomite vs. limestone," *Chemical Engineering Journal*, vol. 231, pp. 544 – 549, 2013.

[28] J. Ylatalo, J. Parkkinen, J. Ritvanen, T. Tynjala, and T. Hyppanen, "Modeling of the oxy-combustion calciner in the post-combustion calcium looping process," *Fuel*, vol. 113, pp. 770–779, 2013.

[29] N. Rodriguez, M. Alonso, J. C. Abanades, A. Charitos, C. Hawthorne, G. Scheffknecht, D. Y. Lu, and E. J. Anthony, "Comparison of experimental results from three dual fluidized bed test facilities capturing CO_2 with CaO," *Energy Procedia*, vol. 4, pp. 393 – 401, 2011.

[30] F. Pontiga, J. M. Valverde, H. Moreno, and F. J. Duran-Olivencia, "Dry gassolid carbonation in fluidized beds of $Ca(OH)_2$ and nanosilica/$Ca(OH)_2$ at ambient temperature and low CO_2 pressure," *Chemical Engineering Journal*, vol. 222, pp. 546 – 552, 2013.

[31] L. M. Romeo, Y. Lara, P. Lisbona, and A. Martinez, "Economical assessment of competitive enhanced limestones for CO_2 capture cycles in power plants," *Fuel Processing Technology*, vol. 90, no. 6, pp. 803 – 811, 2009.

[32] I. Martnez, G. Grasa, R. Murillo, B. Arias, and J. Abanades, "Modelling the continuous calcination of $CaCO_3$ in a Ca-looping system," *Chemical Engineering Journal*, vol. 215-216, pp. 174–181, 2013.

[33] B. Arias, G. S. Grasa, M. Alonso, and J. C. Abanades, "Post - combustion calcium looping process with a highly stable sorbent activity by recarbonation," *Energy Environ. Sci.*, vol. 5, pp. 7353 – 7359, 2012.

[34] M. E. Diego, B. Arias, M. Alonso, and J. C. Abanades, "The impact of calcium sulfate and inert solids accumulation in post-combustion calcium looping systems," *Fuel*, vol. 109, pp. 184 – 190, 2013.

[35] G. Grasa, I. Martnez, M. E. Diego, and J. C. Abanades, "Determination of CaO carbonation kinetics under recarbonation conditions," *Energy & Fuels*, vol. 28, no. 6, p. 4033 4042, 2014.

[36] J. M. Valverde, P. E. Sanchez Jimenez, and L. A. Perez Maqueda, "High and stable CO_2 capture capacity of natural limestone at Ca-looping conditions by heat pretreatment and recarbonation synergy," *Fuel*, vol. 123, pp. 79–85, 2014.

[37] J. M. Valverde, P. E. Sanchez-Jimenez, and L. A. Perez-Maqueda, "Effect of heat pretreatment/recarbonation in the Ca-looping process at realistic calcination conditions," *Energy & Fuels*, vol. 28, no. 6, pp. 4062–4067, 2014.

[38] M. Alonso, Y. Criado, J. Abanades, and G. Grasa, "Undesired effects in the determination of CO_2 carrying capacities of CaO during TG testing," *Fuel*, vol. 127, pp. 52–61, 2014.

692 [39] F. Garcia-Labiano, A. Abad, L. de Diego, P. Gayan, and J. Adanez, "Calcination of calcium-
693 based sorbents at pressure in a broad range of CO_2 concentrations," *Chemical Engineering*
694 *Science*, vol. 57, no. 13, pp. 2381 – 2393, 2002.
695 [40] G. Grasa, R. Murillo, M. Alonso, and J. C. Abanades, "Application of the random pore model
696 to the carbonation cyclic reaction," *AIChE J.*, vol. 55, no. 5, pp. 1246–1255, 2009.
697 [41] G. S. Grasa and J. C. Abanades, "CO_2 capture capacity of CaO in long series of carbona-
698 tion/calcination cycles," *Ind. Eng. Chem. Res.*, vol. 45, no. 26, pp. 8846–8851, 2006.
699 [42] J. M. Valverde, P. E. Sanchez Jimenez, A. Perejon, and L. A. Perez-Maqueda, "CO_2 multicyclic
700 capture of pretreated/doped CaO in the Ca – looping process. Theory and experiments," *Phys.*
701 *Chem. Chem. Phys.*, vol. 15, pp. 11775 – 11793, 2013.
702 [43] J. M. Valverde, "A model on the CaO multicyclic conversion in the Ca-looping process,"
703 *Chemical Engineering Journal*, vol. 228, pp. 1195–1206, 2013.
704 [44] J. Wang, V. Manovic, Y. Wu, and E. J. Anthony, "A study on the activity of CaO-based
705 sorbents for capturing CO_2 in clean energy processes," *Applied Energy*, vol. 87, no. 4, pp. 1453
706 – 1458, 2010.
707 [45] A. Martinez, Y. Lara, P. Lisbona, and L. M. Romeo, "Energy penalty reduction in the calcium
708 looping cycle," *International Journal of Greenhouse Gas Control*, vol. 7, pp. 74 – 81, 2012.
709 [46] P. E. Sanchez-Jimenez, L. A. Perez-Maqueda, and J. M. Valverde, "Nanosilica supported cao:
710 A regenerable and mechanically hard CO_2 sorbent at Ca-looping conditions," *Applied Energy*,
711 vol. 118, pp. 92 – 99, 2014.
712 [47] J. M. Valverde, P. E. Sanchez-Jimenez, L. A. Perez-Maqueda, M. Quintanilla, and J. Perez-
713 Vaquero, "Role of crystal structure on capture by limestone derived CaO subjected to carbon-
714 ation/recarbonation/calcination cycles at Ca-looping conditions," *Applied Energy*, vol. 125,

pp. 264 – 275, 2014.

[48] P. E. Sanchez-Jimenez, J. M. Valverde, and L. A. Perez-Maqueda, "Multicyclic conversion of limestone at Ca-looping conditions: The role of solid-sate diffusion controlled carbonation," *Fuel*, vol. 127, pp. 131 – 140, 2014.

[49] J. M. Valverde, P. E. Sanchez-Jimenez, and L. A. Perez-Maqueda, "On the relevant influence of limestone crystallinity on CO_2 capture in the ca-looping technology at realistic calcination conditions," *Environmental Science & Technology*, vol. 48, no. 16, pp. 9882–9889, 2014.

[50] R. A. W. Haul and H. Heystek, "Differential thermal analysis of the dolomite decomposition," *American Mineralogist*, vol. 37, no. 3–4, pp. 166–179, 1952.

[51] P. Caceres and E. Attiogbe, "Thermal decomposition of dolomite and the extraction of its constituents," *Minerals Engineering*, vol. 10, no. 10, pp. 1165 – 1176, 1997.

[52] E. P. Hyatt, I. B. Cutler, and M. E. Wadsworth, "Calcium carbonate decomposition in carbon dioxide atmosphere," *Journal of the American Ceramic Society*, vol. 41, no. 2, pp. 70–74, 1958.

[53] D. Beruto, L. Barco, and A. W. Searcy, "CO_2-catalyzed surface area and porosity changes in high-surface-area CaO aggregates," *Journal of the American Ceramic Society*, vol. 67, no. 7, pp. 512–516, 1984.

[54] Y. Wang and W. J. Thomson, "The effects of steam and carbon dioxide on calcite decomposition using dynamic X-ray diffraction," *Chemical Engineering Science*, vol. 50, no. 9, pp. 1373 – 1382, 1995.

[55] J. Khinast, G. Krammer, C. Brunner, and G. Staudinger, "Decomposition of limestone: The influence of CO_2 and particle size on the reaction rate," *Chemical Engineering Science*, vol. 51, no. 4, pp. 623–634, 1996.

[56] D. Beruto, A. W. Searcy, and M. G. Kim, "Microstructure, kinetic, structure, thermodynamic analysis for calcite decomposition: free-surface and powder bed experiments," *Thermochimica Acta*, vol. 424, no. 1 2, pp. 99 – 109, 2004.

[57] B. Stanmore and P. Gilot, "Review - calcination and carbonation of limestone during thermal cycling for CO_2 sequestration," *Fuel Processing Technology*, vol. 86, no. 16, pp. 1707 – 1743, 2005.

[58] I. Martinez, G. Grasa, R. Murillo, B. Arias, and J. C. Abanades, "Kinetics of calcination of partially carbonated particles in a Ca-looping system for CO_2 capture," *Energy & Fuels*, vol. 26, no. 2, pp. 1432–1440, 2012.

[59] D. Dollimore, J. Dunn, Y. Lee, and B. Penrod, "The decrepitation of dolomite and limestone," *Thermochimica Acta*, vol. 237, no. 1, pp. 125 – 131, 1994.

[60] M. Samtani, E. Skrzypczak-Janktun, D. Dollimore, and K. Alexander, "Thermal analysis of ground dolomite, confirmation of results using an X-ray powder diffraction methodology," *Thermochimica Acta*, vol. 367–368, pp. 297 – 309, 2001.

[61] D. Beruto, R. Vecchiattini, and M. Giordani, "Effect of mixtures of H_2O (g) and CO_2 (g) on the thermal half decomposition of dolomite natural stone in high CO_2 pressure regime," *Thermochimica Acta*, vol. 404, no. 1–2, pp. 25 – 33, 2003.

[62] R. H. Borgwardt, "Calcium oxide sintering in atmospheres containing water and carbon dioxide," *Industrial & Engineering Chemistry Research*, vol. 28, no. 4, pp. 493 – 500, 1989.

[63] D. Beruto and A. W. Searcy, "Use of the langmuir method for kinetic studies of decomposition reactions: calcite (caco3)," *J. Chem. Soc., Faraday Trans. 1*, vol. 70, pp. 2145–2153, 1974.

[64] S. Dash, M. Kamruddin, P. Ajikumar, A. Tyagi, and B. Raj, "Nanocrystalline and metastable phase formation in vacuum thermal decomposition of calcium carbonate," *Thermochimica*

760 *Acta*, vol. 363, no. 1-2, pp. 129–135, 2000.

761 [65] C. Rrodriguez-Navarro, E. Ruiz-Agudo, A. Luque, A. B. Navarro, and M. Ortega-Huertas,
762 "Thermal decomposition of calcite: Mechanisms of formation and textural evolution of cao
763 nanocrystals," *American Mineralogist*, vol. 94, p. 578 593, 2009.

764 [66] H.-Y. Xie and D. Geldart, "Fluidization of FCC powders in the bubble-free regime: effect
765 types of gases and temperature," *Powder Technol.*, vol. 82, pp. 269 – 277, 1995.

766 [67] C. Luo, Y. Zheng, J. Guo, and B. Feng, "Effect of sulfation on CO_2 capture of CaO-based
767 sorbents during calcium looping cycle," *Fuel*, vol. 127, pp. 124 – 130, 2014.

768 [68] E. O'Neill, D. Keairns, and W. Kittle, "A thermogravimetric study of the sulfation of limestone
769 and dolomitethe effect of calcination conditions," *Thermochimica Acta*, vol. 14, no. 12, pp. 209
770 – 220, 1976.

771 [69] N. Ulerich, E. O'Neill, and D. Keairns, "A thermogravimetric study of the effect of pore
772 volume - pore size distribution on the sulfation of calcined limestone," *Thermochimica Acta*,
773 vol. 26, no. 1 3, pp. 269 – 282, 1978.

774 [70] J. Agnew, E. Hampartsoumian, J. Jones, and W. Nimmo, "The simultaneous calcination and
775 sintering of calcium based sorbents under a combustion atmosphere," *Fuel*, vol. 79, no. 12,
776 pp. 1515 – 1523, 2000.

777 [71] M. E. Diego, B. Arias, G. S. Grasa, and J. C. Abanades, "Design of a novel fluidized bed
778 reactor to enhance sorbent performance in CO_2 capture systems using CaO," *Industrial &*
779 *Engineering Chemistry Research*, vol. 53, no. 24, p. 10059 10071, 2014.

780 [72] R. McCauley and L. Johnson, "Decrepitation and thermal decomposition of dolomite," *Ther-*
781 *mochimica Acta*, vol. 185, no. 2, pp. 271 – 282, 1991.

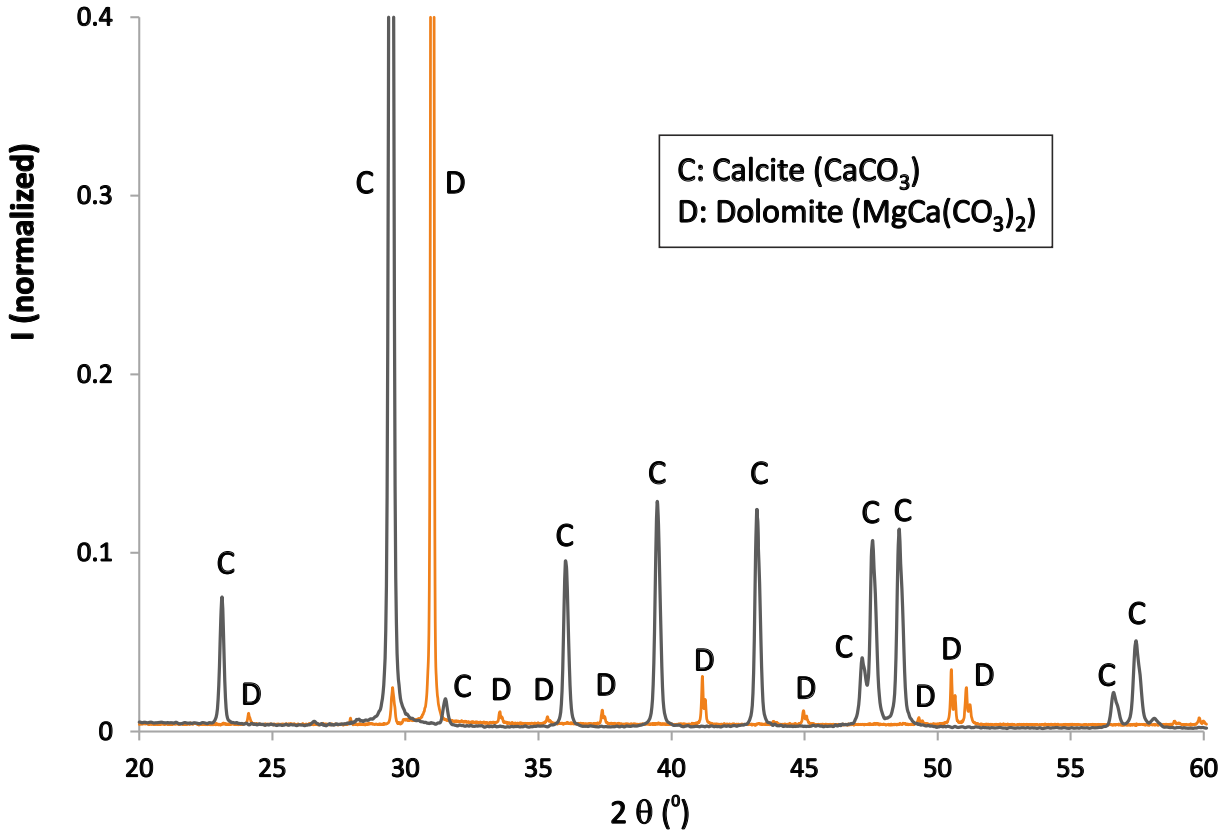

FIG. 1: X-Ray diffractograms measured for samples of dolomite and limestone used in our study (obtained using a Bruker D8 Advance powder diffractometer, Cu-Kα). Values of Intensity are shown normalized to the maximum.

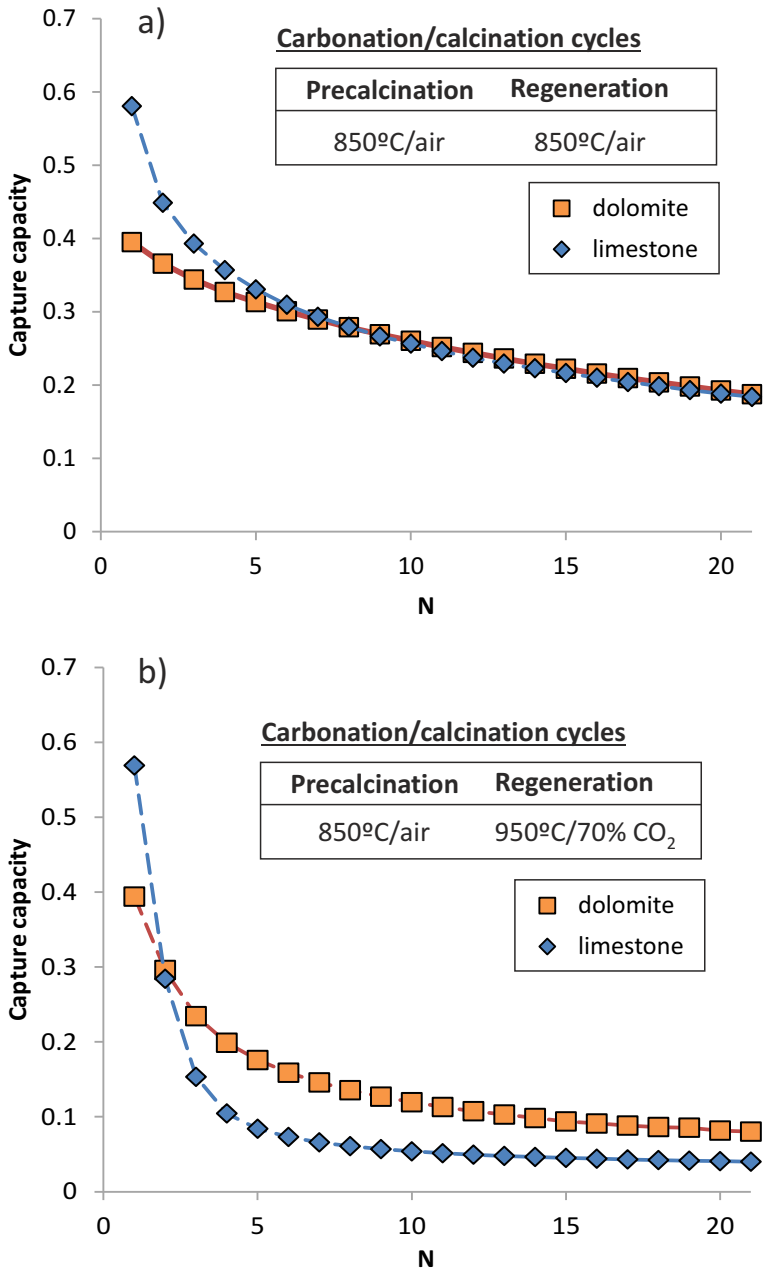

FIG. 2: CO_2 capture capacity as a function of carbonation/calcination cycle number for dolomite and limestone samples precalcined in air and regenerated by calcination either in air at 850°C (a) or under 70%CO_2 at 950°C (b).

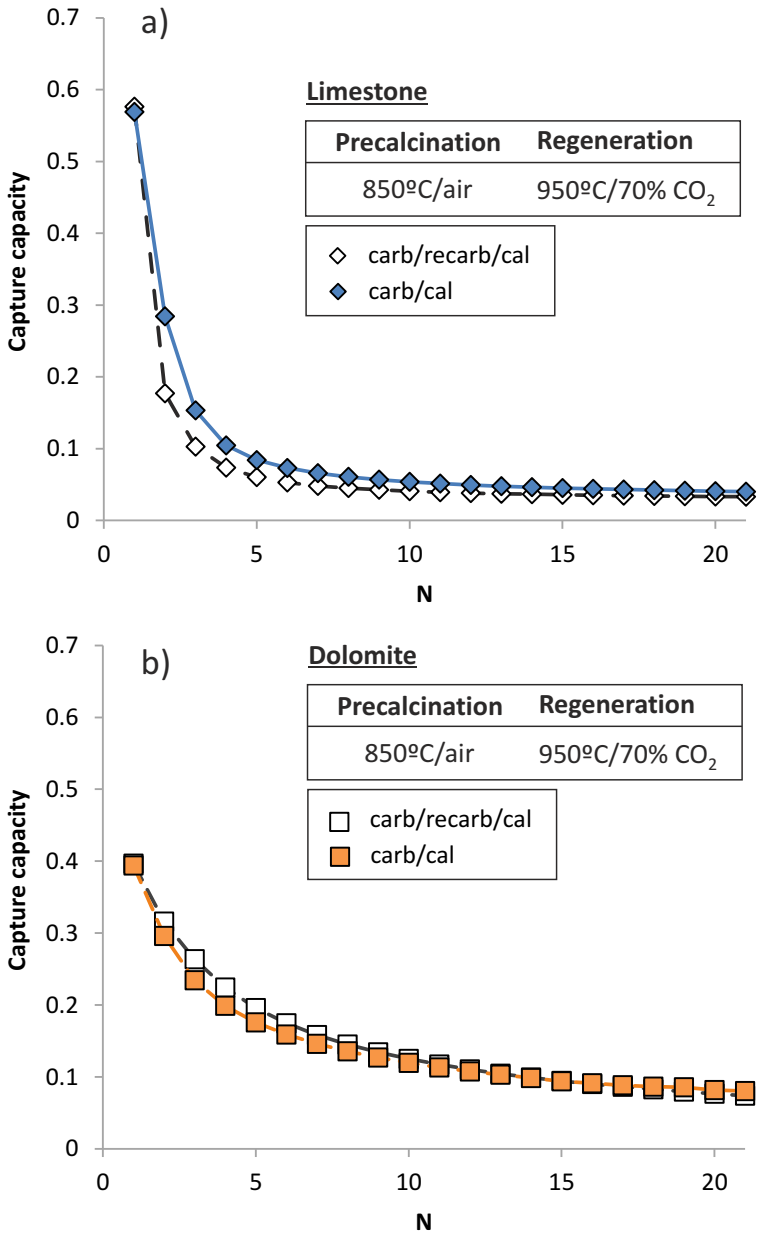

FIG. 3: CO_2 capture capacity as a function of cycle number for limestone (a) and dolomite (b) samples subjected to carbonation/calcination and carbonation/recarbonation/calcination cycles (as indicated), precalcined in air and regenerated by calcination under 70%CO_2 at 950°C.

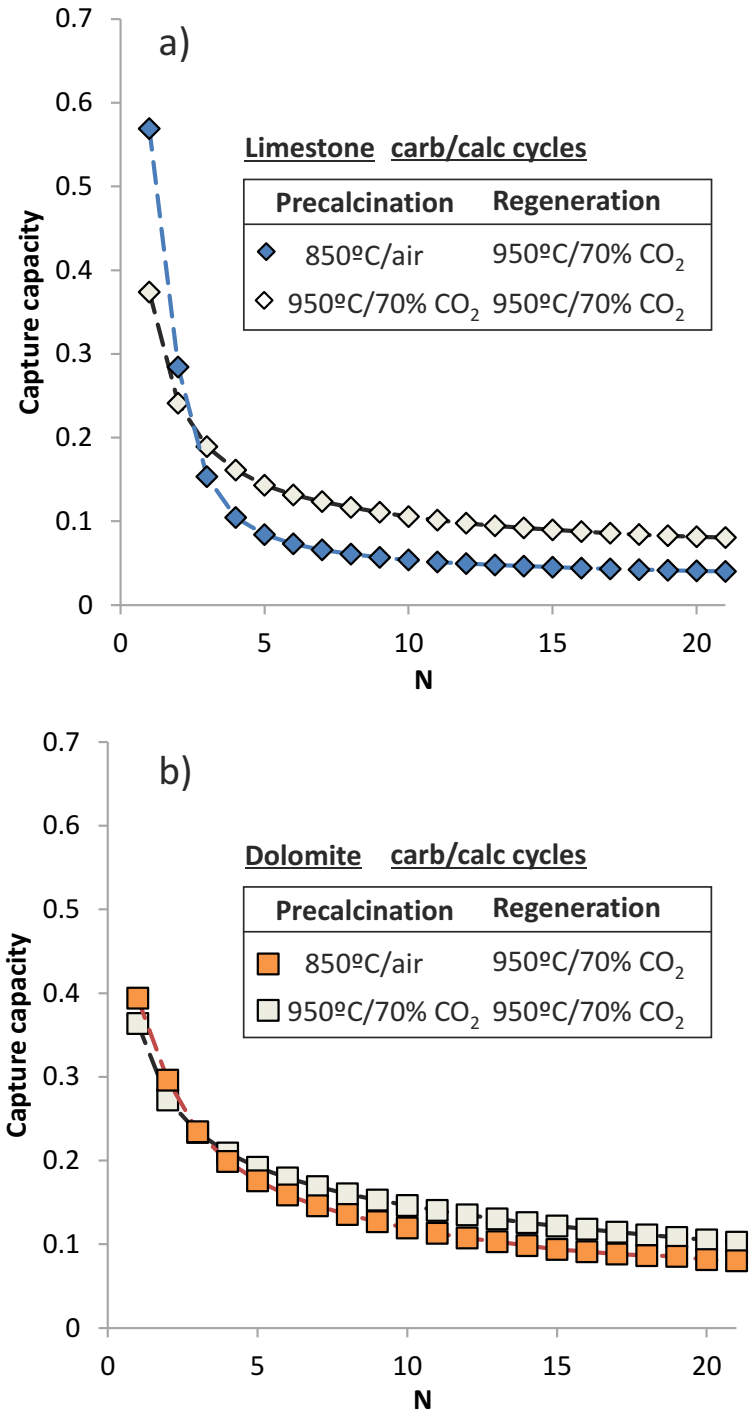

FIG. 4: CO_2 capture capacity as a function of cycle number for limestone (a) and dolomite (b) samples precalcined under different conditions (as indicated) and subjected to carbonation/calcination cycles (regenerated by calcination under 70%CO_2 at 950°C).

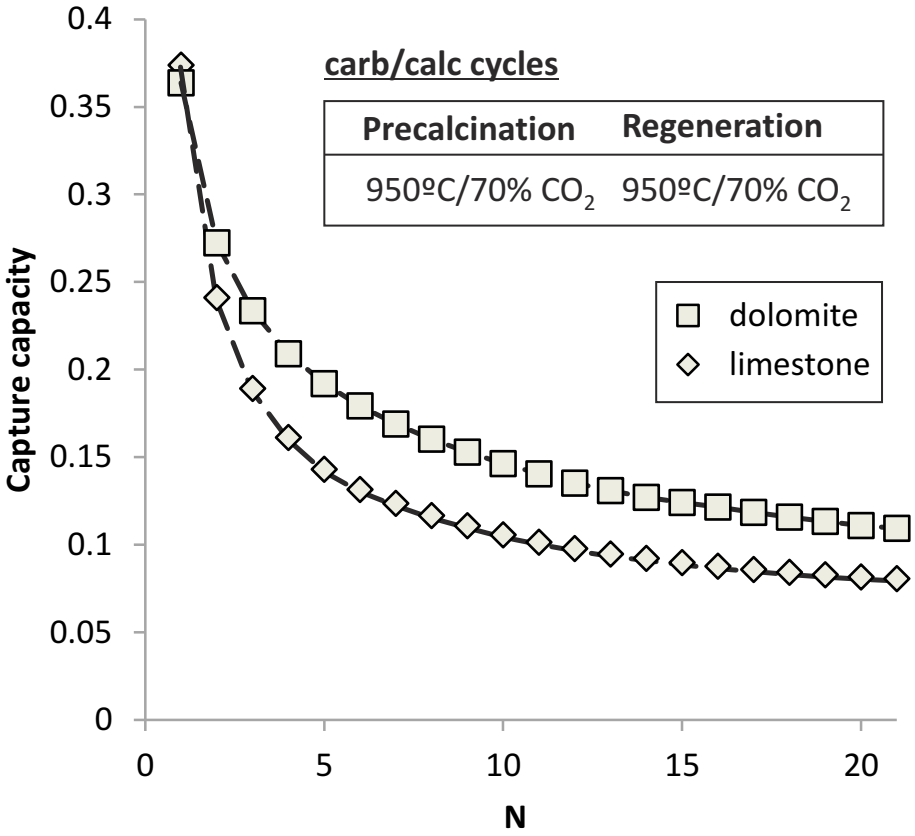

FIG. 5: CO_2 capture capacity as a function of cycle number for limestone and dolomite samples subjected to carbonation/calcination cycles, precalcined and regenerated by calcination under 70%CO_2 at 950°C.

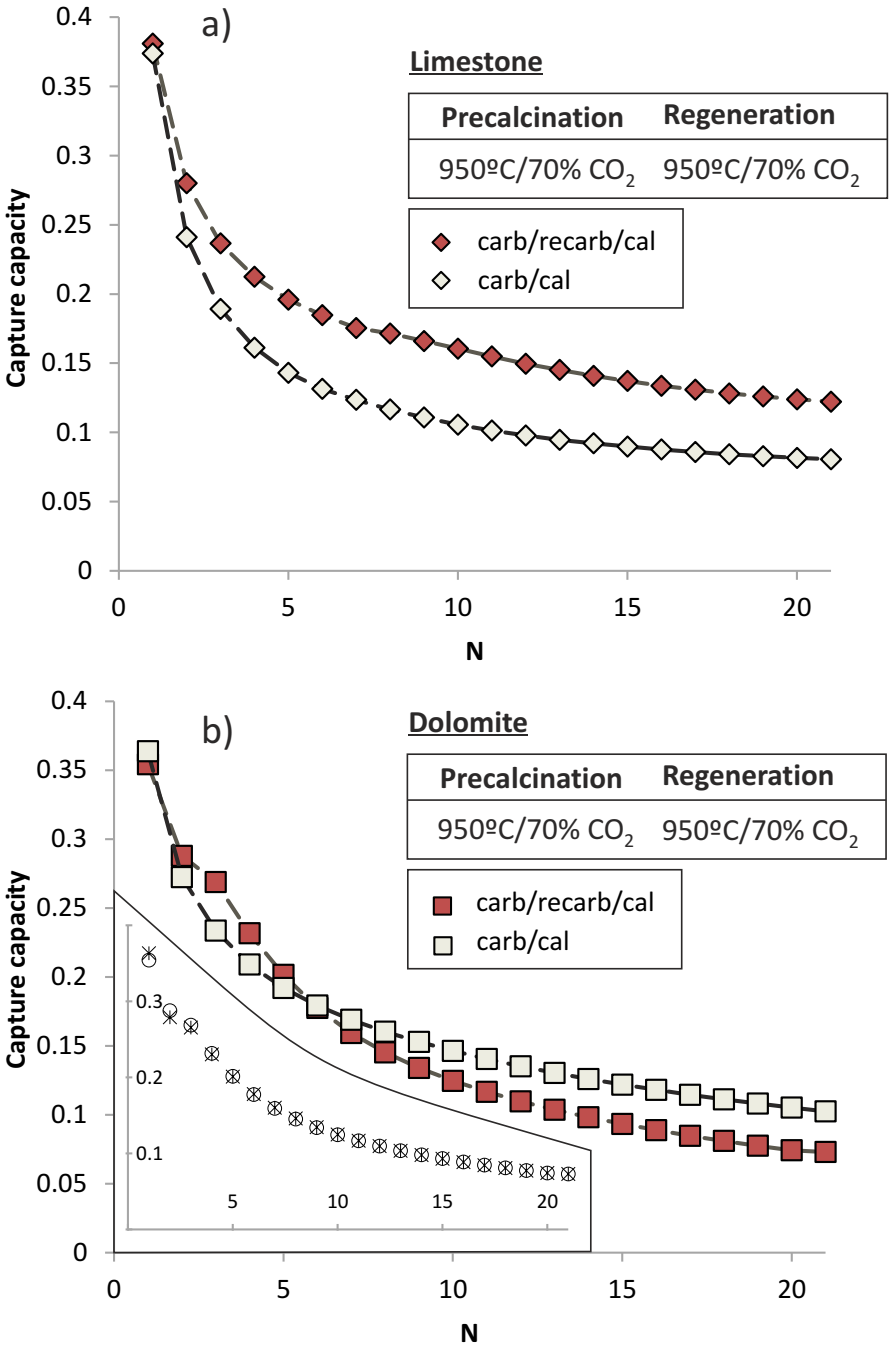

FIG. 6: CO_2 capture capacity as a function of cycle number for limestone (a) and dolomite (b) samples subjected to carbonation/calcination and carbonation/recarbonation/calcination cycles (as indicated) precalcined and regenerated by calcination under 70%CO_2 at 950°C. The inset in b) is a plot of data obtained from tests on different samples of dolomite and same conditions (carb/recarb/calc) to demonstrate results reproducibility.

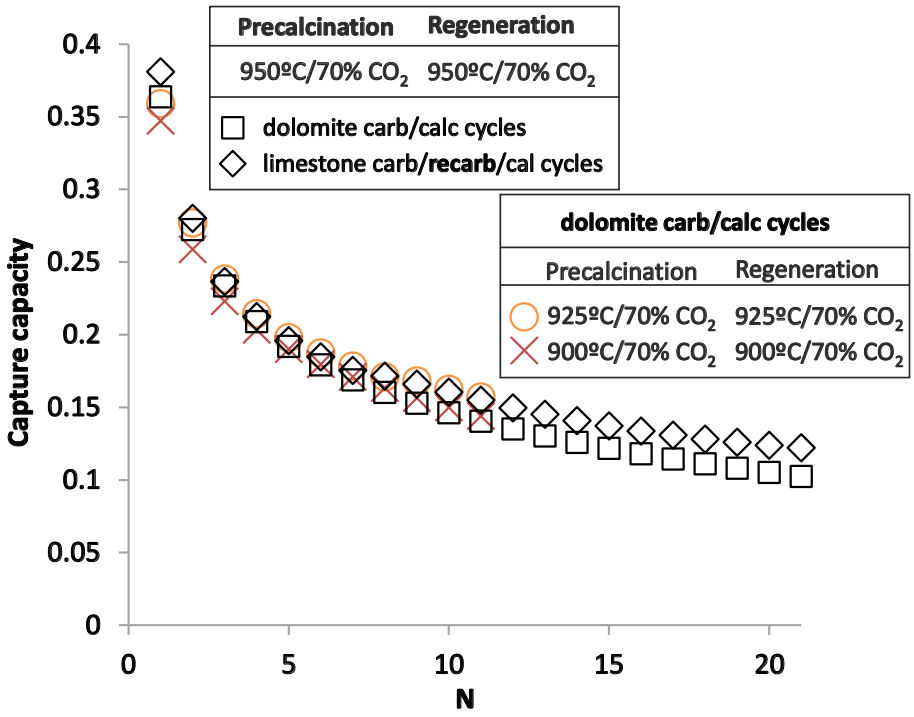

FIG. 7: CO_2 capture capacity as a function of cycle number for dolomite (carbonation/calcination cycles) and limestone samples (carbonation/recarbonation/calcination cycles) precalcined and regenerated by calcination under 70%CO_2 at 950°C. Results for dolomite samples precalcined and regenerated under 70%CO_2 at 925°C and 900°C are also shown.

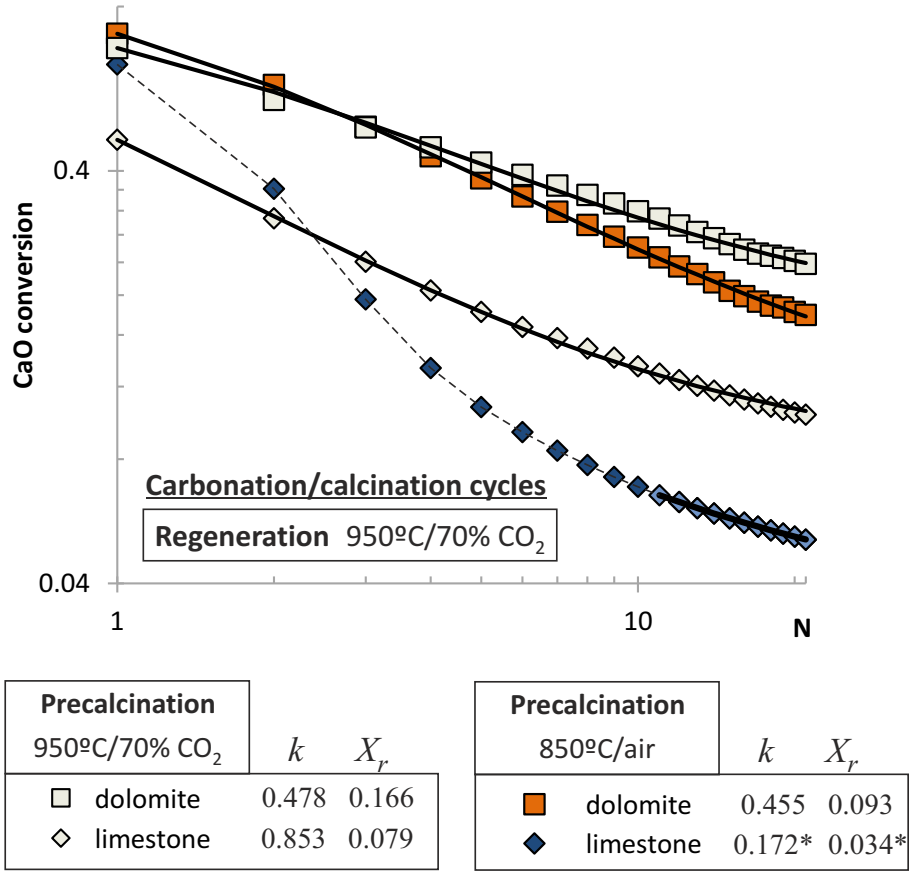

FIG. 8: CaO conversion as a function of cycle number (carbonation/calcination cycles) for dolomite and limestone samples regenerated by calcination under 70%CO_2 at 950°C and precalcined as indicated. The solid lines are drawn from the best fits of Eq. 1 to the data. The inset shows the best fitting parameters (deactivation rate k and residual conversion X_r). (*) In the case of limestone precalcined in air, Eq. 1 fits satisfactorily to the data only from the 10th cycle.

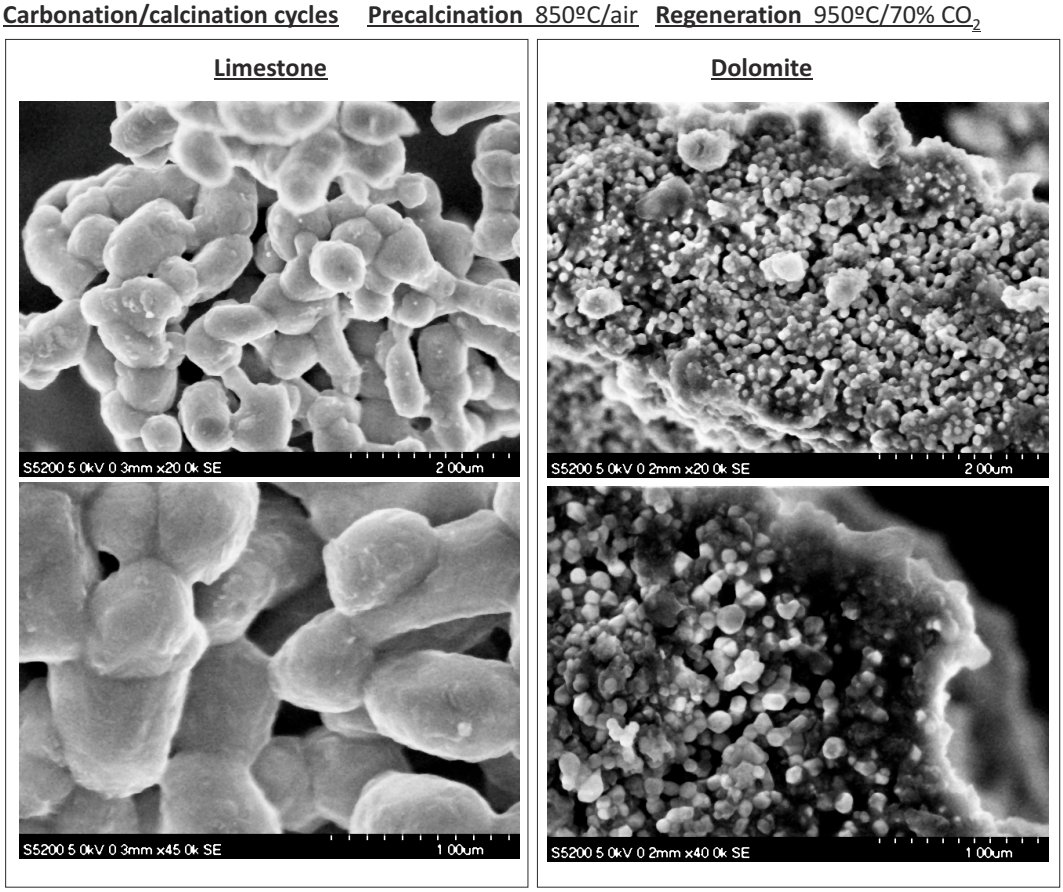

FIG. 9: SEM pictures of limestone and dolomite samples after being subjected to carbonation/calcination cycles (precalcined in air (850°C) and regenerated by calcination under 70%CO_2 at 950°C).

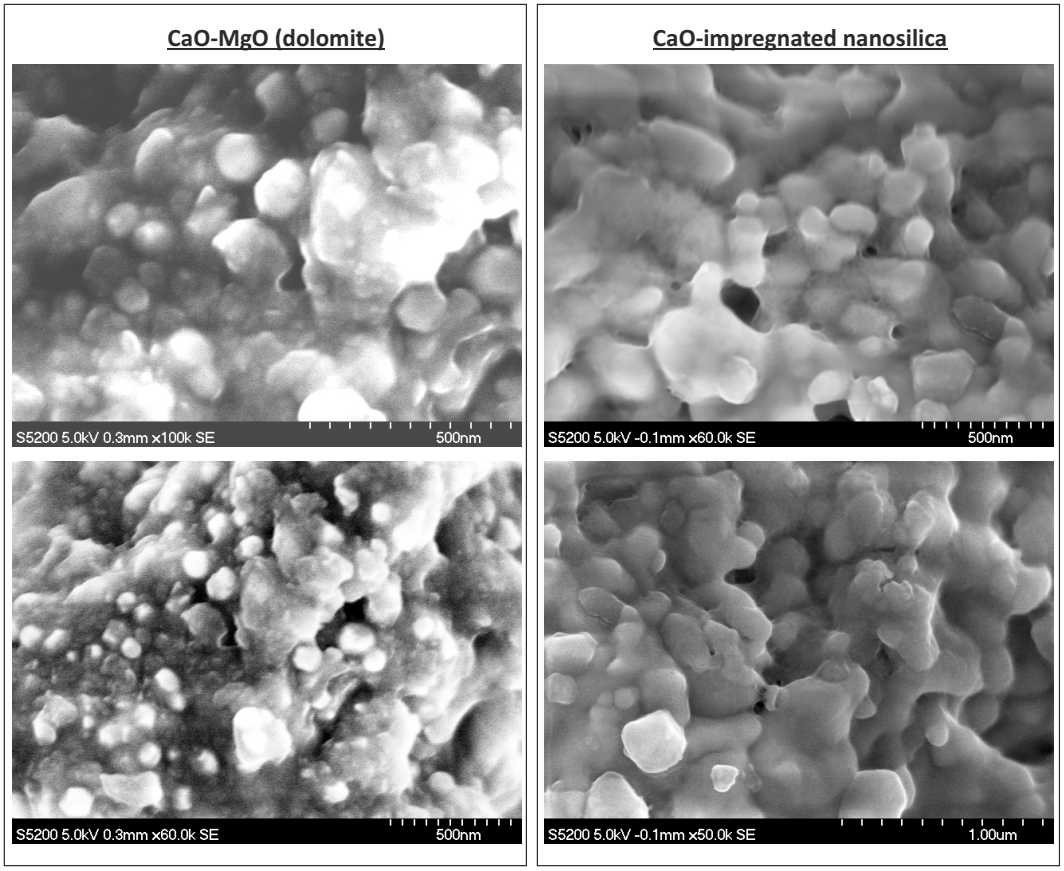

FIG. 10: SEM pictures of: a) dolomite sample after being subjected to carbonation/calcination cycles (regenerated by calcination under 70%CO_2 at 950°C and precalcined in air at 850°C); b) CaO-based sorbent synthesized by impregnation of calcium nitrate solution on a nanostructured calcium silicate matrix after calcination (reported in [46]).

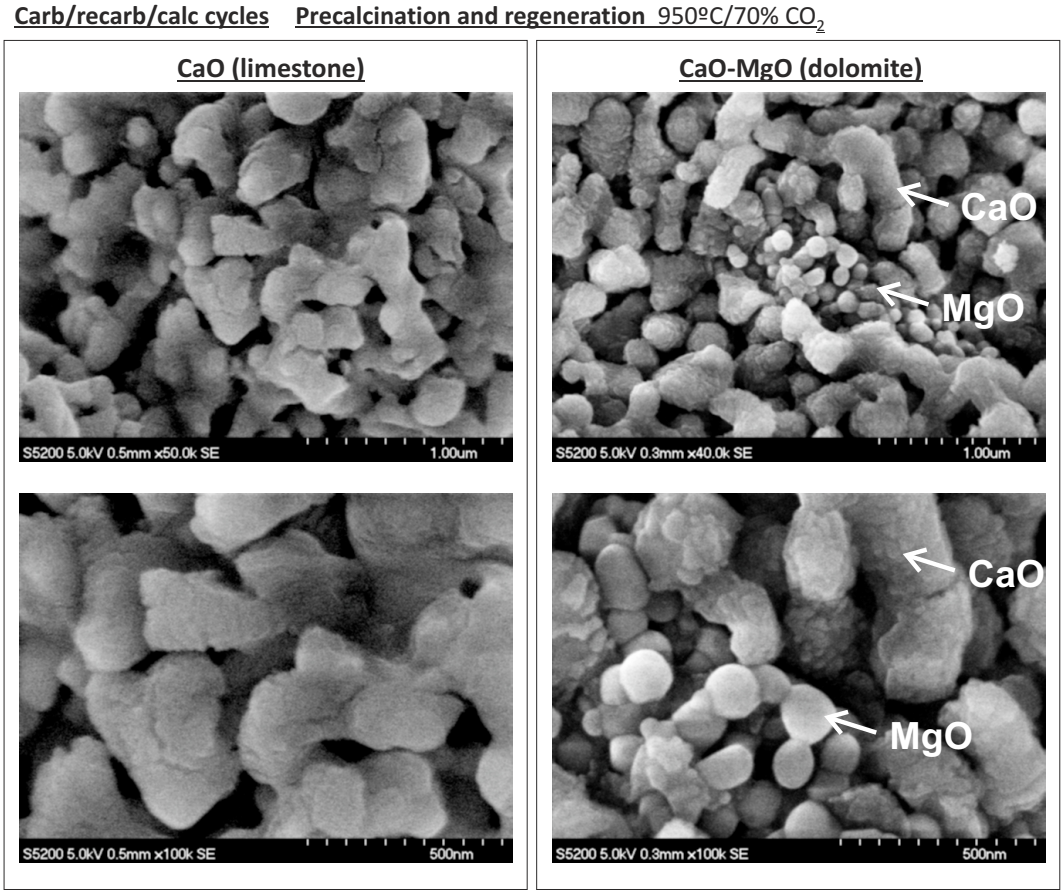

FIG. 11: SEM pictures of limestone and dolomite samples after being subjected to carbonation/recarbonation/calcination cycles (precalcined and regenerated by calcination under 70%CO_2 at 950°C).

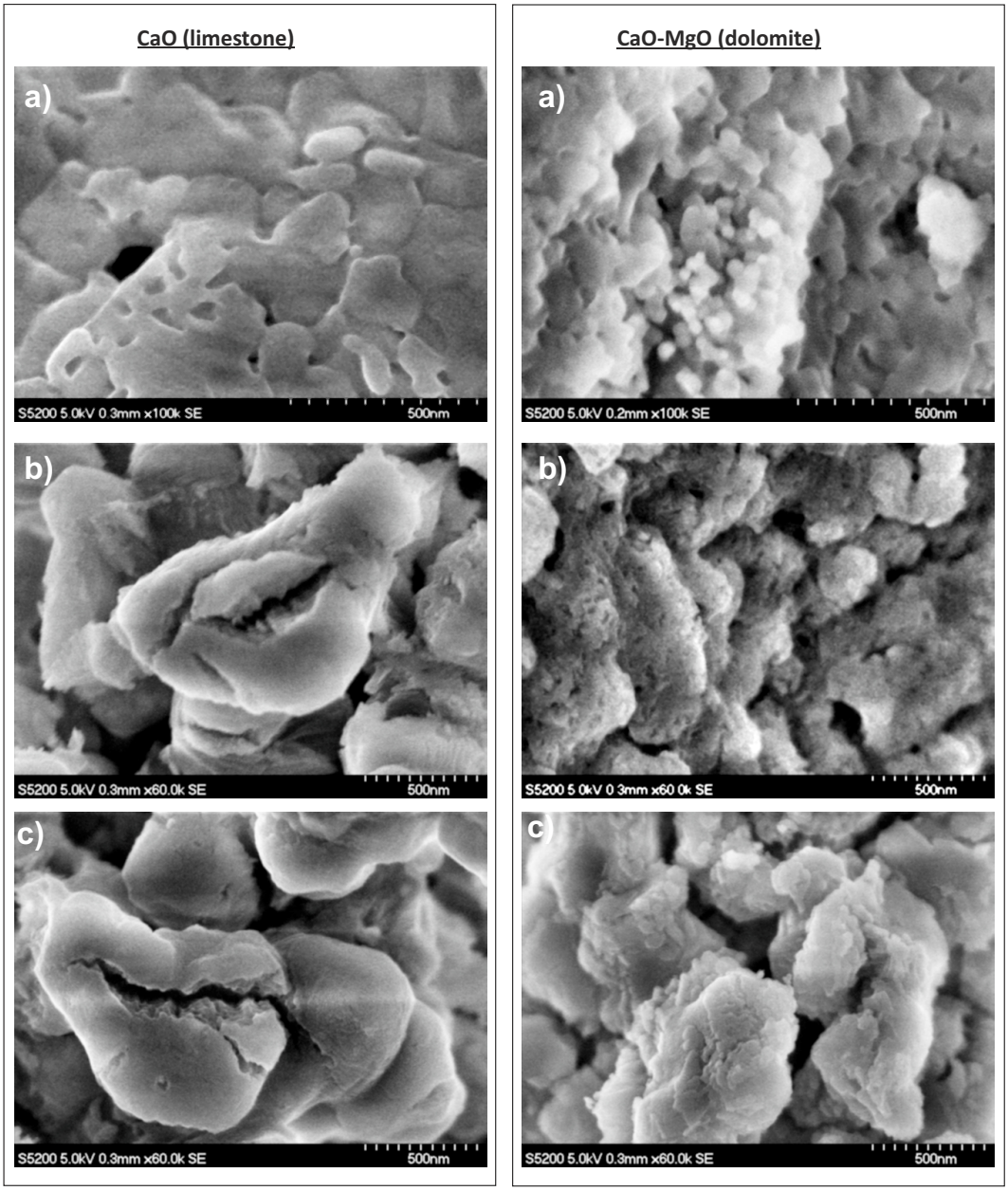

FIG. 12: SEM pictures of limestone and dolomite samples after being cycled under diverse conditions. a) Carbonation/calcination cycles (precalcined and regenerated by calcination in air at 850°C). b) Carbonation/recarbonation/calcination cycles (precalcined and regenerated by calcination under 70%CO_2 at 950°C). c) Carbonation/calcination cycles (precalcined and regenerated by calcination under 70%CO_2 at 950°C).

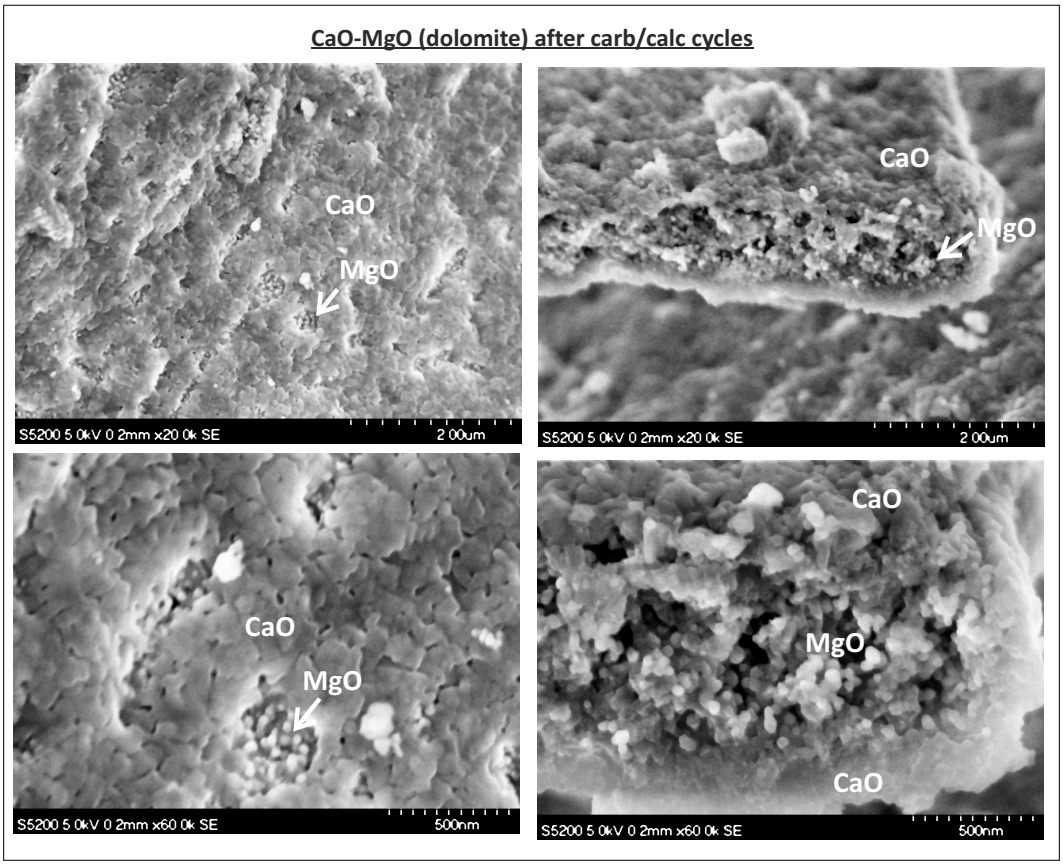

FIG. 13: SEM pictures of a dolomite sample after being subjected to carbonation/calcination cycles (precalcined and regenerated by calcination in air at 850°C).

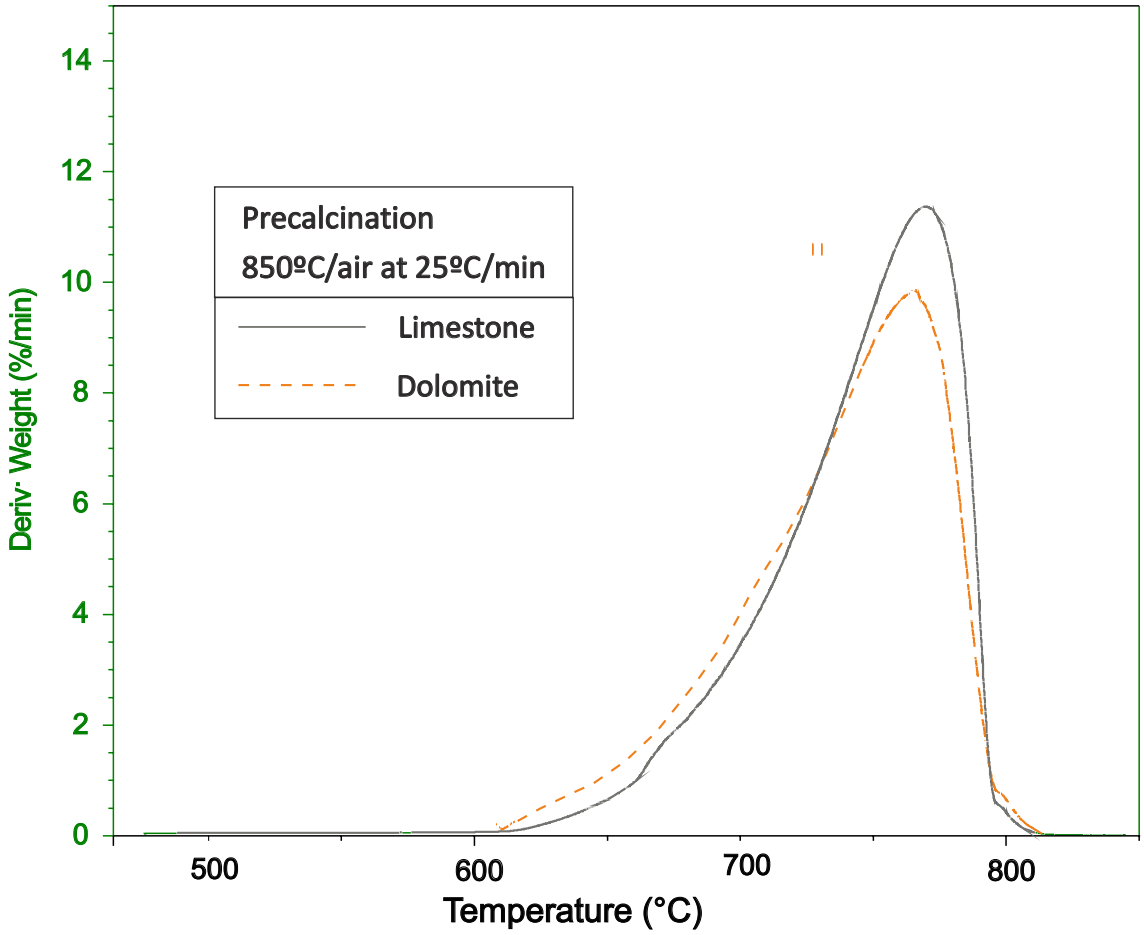

FIG. 14: Derivative of sample weight % (absolute value) as a function of temperature during decomposition of samples of dolomite and limestone precalcined in-situ in the TGA tests under air by slowly increasing the temperature up to 850°C).

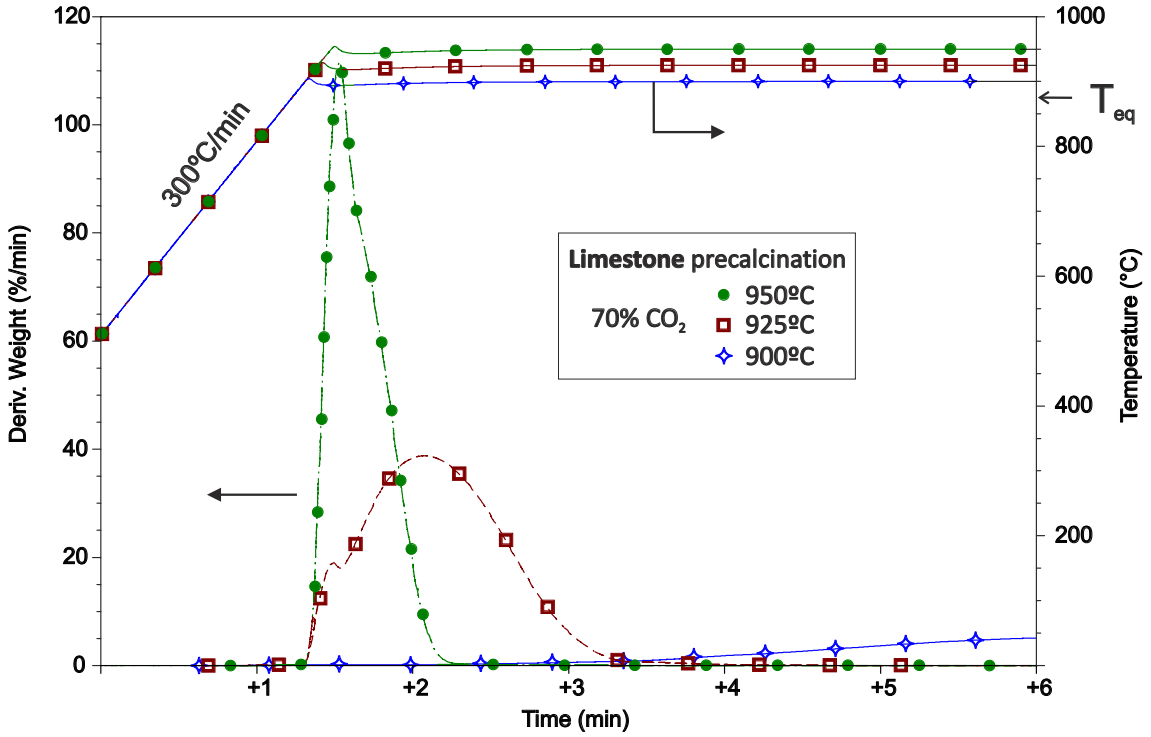

FIG. 15: Time evolution of sample weight % derivative (absolute value) and temperature during decomposition of samples of limestone precalcined in-situ in the TGA tests under 70%CO_2 by quickly increasing the temperature up to 900°C, 925°C, and 950°C (as indicated). The arrow in the temperature axis (right) indicates the thermodynamic equilibrium temperature ($T_{eq} \approx 870$°C).

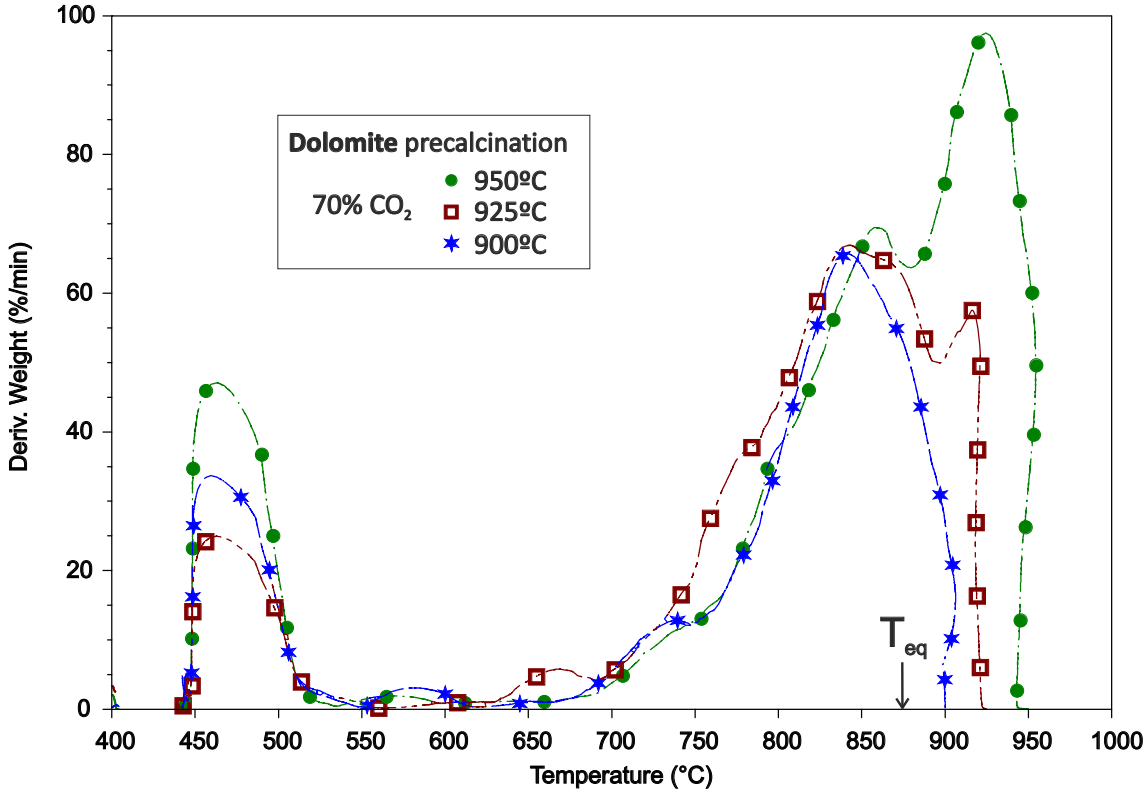

FIG. 16: Derivative of sample weight % (absolute value) as a function of temperature during decomposition of samples of dolomite precalcined under 70%CO_2 in-situ in the TGA tests by quickly increasing the temperature up to 900°C, 925°C, and 950°C (as indicated). The arrow in the temperature axis (horizontal) indicates the thermodynamic equilibrium temperature for pure calcite ($T_{eq} \approx 870$°C)

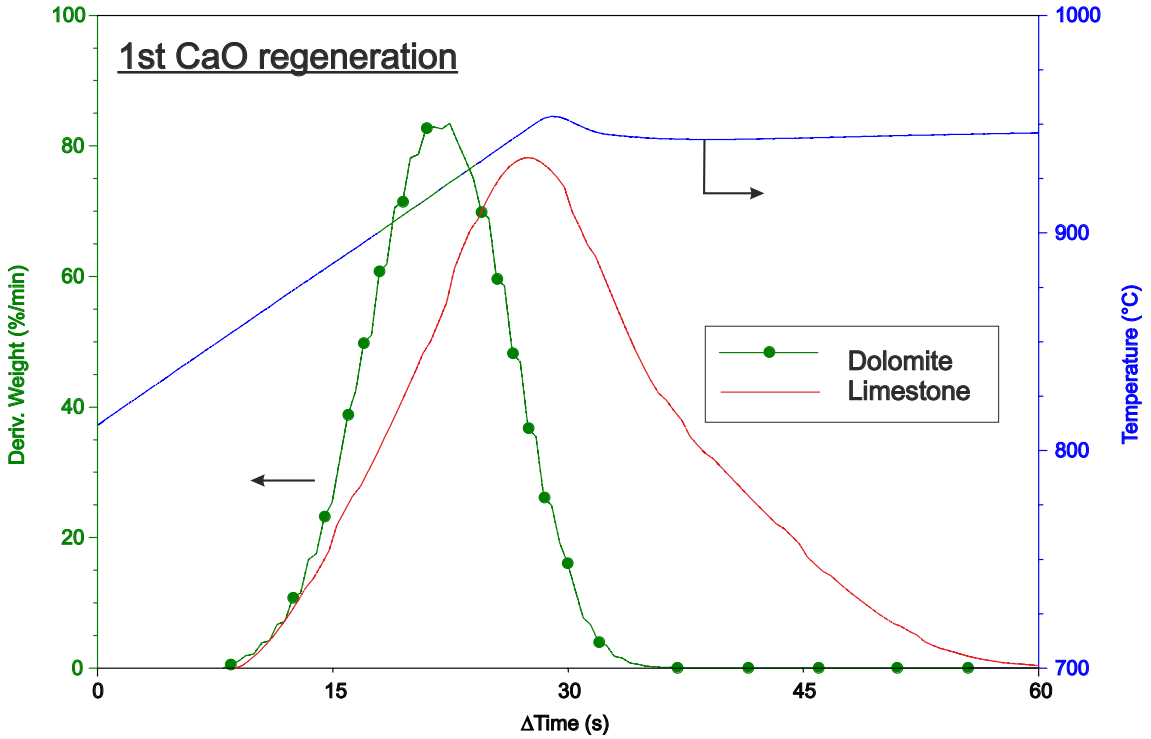

FIG. 17: Time evolution of sample weight % derivative (absolute value) and temperature for samples of limestone and dolomite during 1st regeneration (precalcined and regenerated at 950°C under 70%CO_2) as indicated).

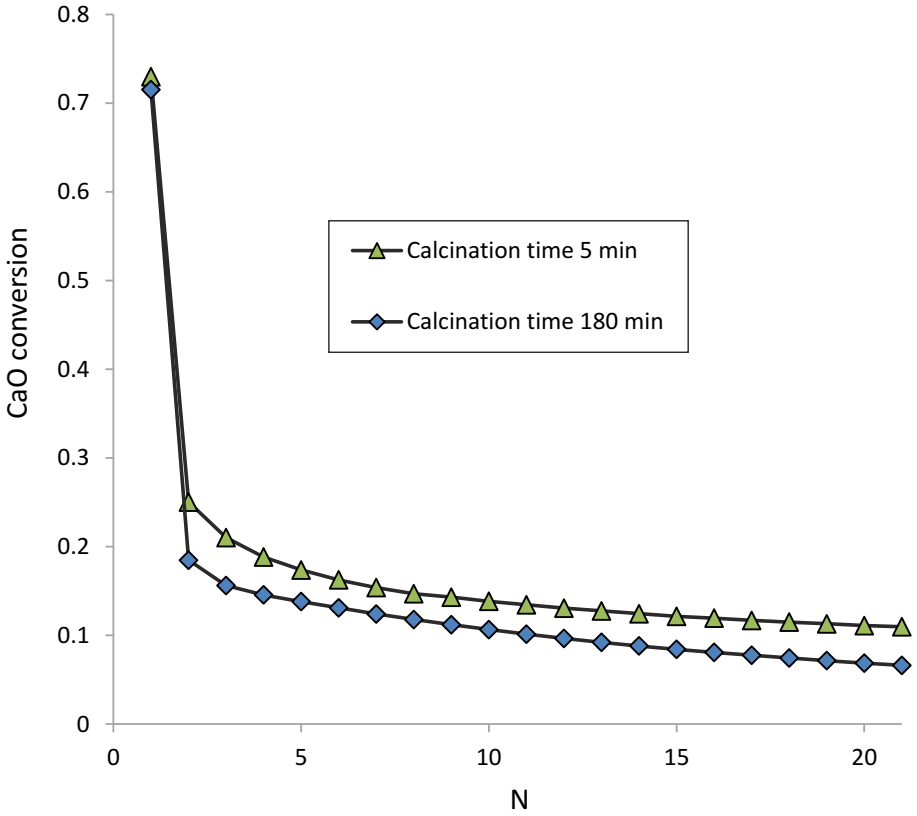

FIG. 18: CaO conversion as a function of cycle number (carbonation/calcination cycles) for limestone samples regenerated by calcination under 70%CO_2 at 925°C (samples precalcined in air at 850°C). Data are shown from tests with different durations of the calcination stages as indicated.